Organic & Biomolecular Chemistry

Tetrathiafulvalene-calix[4]pyrrole: A versatile synthetic receptor for electron-deficient planar and spherical guests

Journal:	*Organic & Biomolecular Chemistry*
Manuscript ID	OB-REV-10-2018-002514.R1
Article Type:	Review Article
Date Submitted by the Author:	26-Jan-2019
Complete List of Authors:	Bähring, Steffen; Department of Chemistry, SDU: Odense University Root, Harrison; The University of Texas at Austin, Dept. of Chemistry and Biochemistry Sessler, Jonathan; The University of Texas at Austin, Dept. of Chemistry and Biochemistry Jeppesen, Jan Oskar; Department of Chemistry, SDU: Odense University

Journal Name

ARTICLE

Tetrathiafulvalene-calix[4]pyrrole: A versatile synthetic receptor for electron-deficient planar and spherical guests

Steffen Bähring,[a]* Harrison D. Root,[b] Jonathan L. Sessler[b]* and Jan O. Jeppesen[a]*

Received 00th January 20xx,
Accepted 00th January 20xx

DOI: 10.1039/x0xx00000x

www.rsc.org/

The first tetrakis-tetrathiafulvalene-calix[4]pyrrole (TTF-C[4]P) was reported in 2004. Early on it and related π-extended TTF-C[4]Ps were found to function as both anion receptors and as hosts for planar electron deficient planar neutral guests, including nitroaromatic explosives. Anion binding was found to occur with a 1:1 binding stoichiometry and to stabilise the cone C[4]P conformation, whereas planar electron deficient guests were bound in a cooperative 1:2 fashion to the 1,3-alternate conformer. Addition of strongly complexing anions was found to trigger release of the electron deficient guests concurrent with a conformational change to the cone form. Subsequent studies led to the discovery of anion-induced complexation with C_{60}, and the finding that the resulting complexes would support fast photoinduced electron-transfer events. Synthetic advances then led to the preparation of nonsymmetric TTF-C[4]Ps where a single moiety organises the receptor in either the 1,3-alternate conformation or the partial cone conformation, thus modifying both selectivity and sensitivity. TTF-C[4]P-based stimulus responsive systems, that rely on anions and cations as controlling inputs, have also been developed and studied in recent years. This review provides a summary of TTF-C[4]P-related chemistry.

Introduction

Late in the 20th century, Becher and Jeppesen reported the first tetrathiafulvalene (TTF) annulated pyrrole derivative constructed from **1**[1,2] (Fig. 1). This precursor allowed TTF redox reactivity to be combined with calix[4]pyrrole-based anion recognition, thus fusing two important branches of supramolecular chemistry. Calix[4]pyrroles (C[4]Ps), in the form of octamethyl-calix[4]pyrrole (**2**, Fig. 1), were originally reported as "pyrrol-aceton" by Bayer[3] by in 1886. In the mid-1990's the ability of this venerable system to function as an anion receptor in organic media was reported by Sessler and Gale.[4] It was found that anion binding induces a change from the dominant 1,3-alternate conformation to the corresponding cone conformation as shown in Fig. 2.

To date, many examples of *meso*-functionalised calix[4]pyrroles have been reported, including strapped calix[4]pyrroles and bis-calix[4]pyrroles.[5-7] Functionalisation of the pyrrole β-positions in C[4]P's has proved more challenging, with only a few examples apart from the TTF-calix[4]pyrroles (TTF-C[4]Ps **3**–**5**) being known.[8-10] The ability to append synthetically a TTF unit onto the β-positions of pyrrole thus provided a key precursor that allowed introduction of redox active TTF subunits into the calix[4]pyrrole framework.

Dibenzo-TTF was first synthesised in 1926 by Hurtley and Smiles.[11] However, it was only after its redox properties were recognised by Wudl[12] and the first organic superconductor

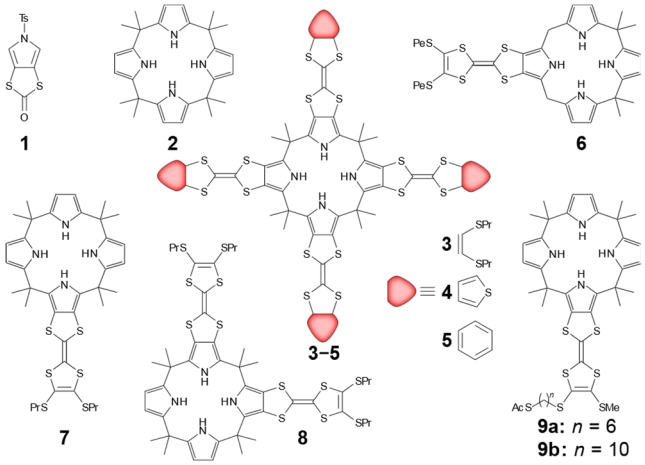

Fig. 1 Chemical structures of TTF- pyrrole precursor **1**, octamethylcalix[4]pyrrole **2**, tetrakis-TTF-calix[4]pyrroles **3**–**5**, mono-TTF-calix[4]pyrroles **6** and **7**, bis-TTF-calix[4]pyrrole **8** and thioacetyl mono-TTF-calix[4]pyrroles **9a**–**b**.

based on TTFs were reported[13-15] that TTF began to attract extensive interest. This led, *inter alia*, to applications in the area of supramolecular chemistry.[16-22] As noted by Becher and coworkers,[16] the redox active features of TTF has led to it being exploited in a range of different research areas, including supramolecular polymers[23-27] and molecular muscles.[28-31]

A number of TTF-containing C[4]P systems are now known. While recent reviews[32,33] cover the chemistry of these systems in broad strokes, no detailed summary of the conformational features and methods for controlling structure and function has been published. In this review, we focus on the evolution TTF-C[4]P receptors in the context of supramolecular chemistry.

The first effective merging of TTF and C[4]P chemistry came in 2003, when Becher and Jeppesen[34] reported the synthesis and anion-binding properties of a mono-TTF C[4]P **6**. This

[a] *Department of Physics, Chemistry and Pharmacy, University of Southern Denmark, Campusvej 55, 5230, Odense M, Denmark. E-mail: sbahring@sdu.dk; joj@sdu.dk; Tel: +45 65 50 25 87*
[b] *Department of Chemistry, The University of Texas at Austin, Austin, Texas 78712-1224, USA. E-mail: Sessler@cm.utexas.edu; Tel: +01 512 471 5009*
† Footnotes relating to the title and/or authors should appear here.

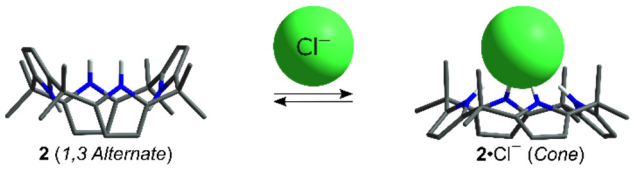

Fig. 2 Change in the dominant conformation seen upon the binding of a chloride anion to octamethyl-calix[4]pyrrole **2**.

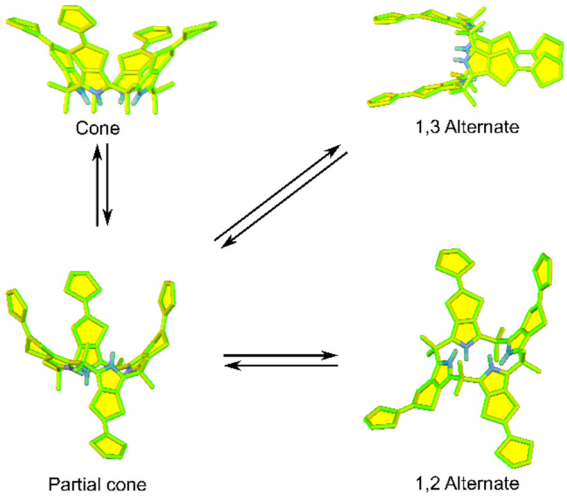

Fig. 3 Cartoon representation of the discrete conformations of TTF-C[4]P.

system bears thiopentyl substituents on the TTF moiety and lacks geminal methyl groups in two of the four *meso*-positions. It was shown to complex halide anions (as their tetrabutylammonium (TBA^+) salts), an interaction that was monitored as a cathodic shift of the first oxidation potential ($E^1_{½}$) by cyclic voltammetry (CV). Anion binding also led to large downfield shifts in the pyrrole NH proton resonances in the ^{1}H NMR spectrum ($\Delta\delta$ = 2.2–3.2 ppm in CD_3CN containing 0.5% v/v D_2O, 300 K). These latter changes could be used to derive the corresponding binding affinities (Table 1).

The fully *meso*-methyl substituted isomers of thiopropyl-substituted TTF, mono- and bis-TTF-calix[4]pyrroles **7** and **8** (Fig. 1) respectively, were later reported by Nielsen *et al*.[35] Increasing the number of TTF moieties led to stronger anion complexation, as well as larger cathodic shifts in the first oxidation potential ($E^1_{½}$). These changes were ascribed to the relative increase in the acidity of the pyrrole NH protons. Both **7** and **8** acted as electrochemical sensors for anions. Subsequently, Jensen *et al*. reported a pair of mono TTF C[4]Ps bearing thioacetyl groups (**9a**–**b**, Fig. 1).[36] Self-assembled monolayers (SAMs) of **9b** were then prepared on a gold surface and used to sense chloride at the sub-millimolar level.

TTF-C[4]P conformational binding behaviour

As true for other C[4]Ps, TTF-C[4]Ps can adopt different conformations (Fig. 3). The dominant conformation in the absence of some external influence is the 1,3-alternate conformation.[37,38] The 1,2-alternate and partial cone are present at ca. 6% and 14%, respectively. There is no appreciable concentration of the cone conformation. However, the latter form dominates in the presence of Lewis basic anions (Fig. 2).

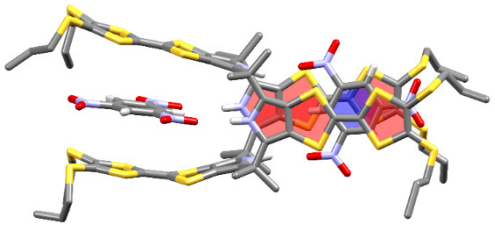

Fig. 4 Crystal structure of the TNB_2⊂**3** complex. All hydrogen atoms except the NH and Ar-H protons have been removed for clarity.[39]

A collaboration between the groups of Jeppesen and Sessler led to the preparation of the first TTF-C[4]P **3**.[39] This compound was initially shown to complex electron-deficient planar guests, including 1,3,5–trinitrobenzene (TNB), tetrafluoro–*p*–benzoquinone, tetrachloro–*p*–benzoquinone and *p*–benzoquinone, in CH_2Cl_2 solution. Easy-to-discern colour changes from yellow to green/brown, attributed to π–π donor–acceptor charge-transfer (CT) interactions, were found to accompany complexation. Diffraction-grade crystals of the TNB_2⊂**3** complex (Fig. 4) revealed a 1:2 complex stoichiometry wherein two molecules of TNB are situated in the two separate binding sites defined by the 1,3-alternate conformer. A 6.80–7.10 Å separation between the tweezers-like TTF subunits and the bound guests is seen, as would be expected for a donor–acceptor CT complex.[40] Each bound TNB molecule is further stabilised by hydrogen bonding interactions between the pyrrole NH protons and the TNB nitro group oxygens. In $CDCl_3$ solution, it was found that the pyrrole NH proton resonance (initially located at δ = 7.10 ppm) shifts downfield ($\Delta\delta$ = +0.69 ppm) upon the addition of two molar equivalents of TNB. A quantitative ^{1}H NMR spectral titration of **3** (2.0 mM in $CDCl_3$ at 298 K) with TNB allowed binding constants of K_1 and K_2 of 23 M^{-1} and 896 M^{-1}, respectively, to be obtained. A prominent colour change from yellow (**3**) to green (TNB_2⊂**3**) was also observed (Fig. 5) upon addition of two equiv. of TNB (colourless). Taken in concert, these findings support the formation of a 1:2 TNB complex that is stabilised by both hydrogen bonding and CT interactions. Addition of five molar equiv. of chloride anion (as its TBA^+ salt) to the green TNB_2⊂**3** complex triggered a colour change back to yellow (Fig. 5c). A corresponding ^{1}H NMR spectroscopic study ($CDCl_3$) revealed that upon the addition TBACl to TNB_2⊂**3**, the pyrrole NH protons were shifted even further downfield (from δ = 7.79 ppm to δ = 10.80 ppm). These spectral shifts were taken as evidence that an anion bound complex, **3**•Cl^-, was being formed concurrent with TNB release.

The conformational stability of the complexes of TTF-C[4]P has shown to greatly favour the anion-binding cone conformer. However, in a recent study the complexation of **3** with 1,4,5,8-naphthalene-tetracarboxylic dianhydride, the complex was found to be strongly bound to the 1,3 alternate conformation ($K_1 = 2.9 \times 10^4$ M^{-1} and $K_2 = 1.0 \times 10^6$ M^{-1}) that addition of TBACl (ten equiv. in $CDCl_3$) did not affect changes to the TTF-C[4]P complex.[41]

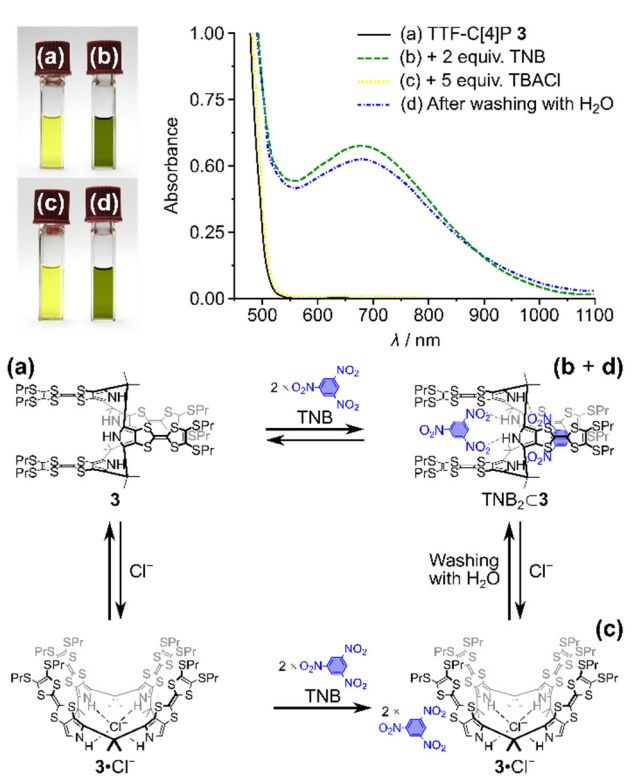

Fig. 5 Top: Absorption spectra (CH_2Cl_2, 298 K) of (a) **3** (1.0 mM), (b) **3** + two equiv. of TNB, (c) **3** + two equiv. of TNB + five equiv. of TBACl and (d) After washing with H_2O. Bottom: Equilibrium scheme occurring in the presence and absence of TNB and TBACl as observed by absorption spectroscopy. Adapted from Ref. 39. Copyright 2004 American Chemical Society.

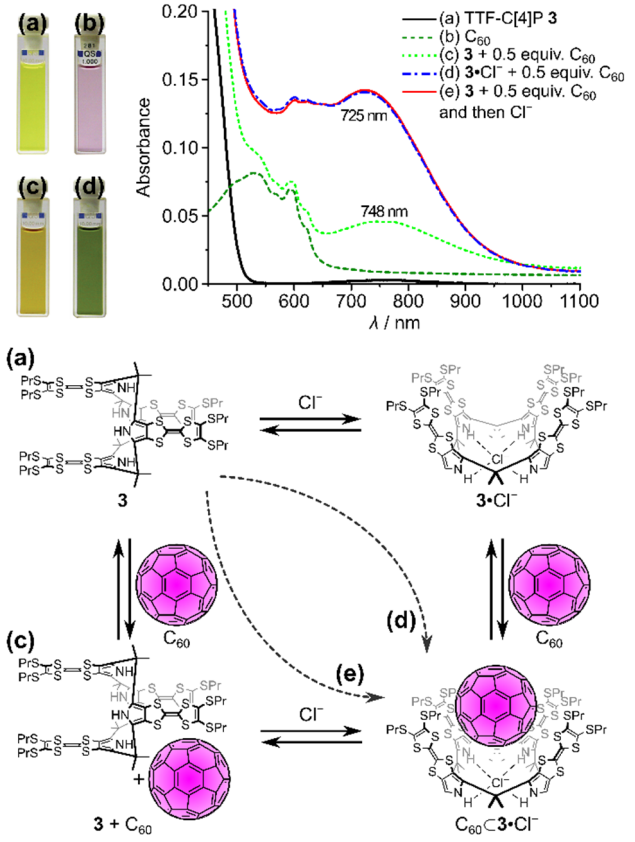

Fig. 6 Top: Absorption spectra (CH_2Cl_2, 298 K) of (a) **3** (0.135 mM), (b) C_{60} (0.0687 mM), (c) **3** + 0.5 equiv. of C_{60}, (d) **3**•Cl^- + 0.5 equiv. of C_{60} and (e) **3** + 0.5 equiv. of C_{60} with excess Cl^- added. Bottom: Equilibrium scheme occurring in the presence and absence of Cl^- and C_{60} as observed by absorption spectroscopy. Adapted from Ref. 42. Copyright 2006 Wiley-VCH Verlag GmbH.

Anion-induced effects

In 2006 Nielsen *et al*. demonstrated that the anion bound cone conformation of TTF-C[4]P **3** would interact with fullerene C_{60} (Fig. 6).[42] When monitoring the change in absorption upon addition of 0.5 equiv. of C_{60} to a solution of **3** (0.135 mM in CH_2Cl_2), a broad absorption feature centred at λ_{max} = 748 nm was observed in the visible spectrum (Fig. 6c). This absorption band is attributed to donor–acceptor CT interactions between the electron-rich TTF units and the electron-poor C_{60}. Upon introduction of five equiv. TBACl to the mixture an increase in the absorption intensity was observed (Fig. 6e), along with a hypsochromic shift in the λ_{max} to 725 nm. This increased absorption was rationalised in terms of a chloride-induced conformational change of **3** to the cone conformation. This switch allows for more efficient interactions between the four TTF units of **3** and the C_{60} guest within the bowl-like cavity of the cone form. Upon reversing the order in which the components are mixed, complex **3**•Cl^- forms first. When this latter species is then exposed to 0.5 equiv. C_{60}, an absorption profile nearly identical to the one formed via the original mixing process is observed. This was interpreted in terms of an analogous complex being formed between the three components. In this original study,[42] the complex stoichiometry was considered to be 1:2 (C_{60}⊂(**3**•Cl^-)$_2$) based on a continuous variation Job plot[43] and a complex solid-state structure inferred from a single crystal X-ray diffraction analysis (Fig. 7a). In fact, a cubic ensemble, consisting of [(TBA⊂**3**•Cl)$_6$(C_{60})$_8$(PhMe)$_5$] was observed in the solid state.[42] After carrying out continuous variation Job plots at varying concentrations of TBACl, it came to be appreciated that a direct reliance on position of the Job plot maxima can be misleading. This is because the chloride-induced equilibrium between the 1,3-alternate- and the cone conformation are also influenced by the presence of the fullerene and the nature and relative concentration of the counter cation. To account for this complexity, Sessler[44] and collaborators constructed modified Job plots wherein the anion concentration was kept constant thereby reducing the effect on the equilibrium between the 1,3-alternate and the cone conformation of **3**. On this basis, a 1:1 binding stoichiometry (C_{60}⊂**3**•Cl^-) was proposed (Fig. 6). A

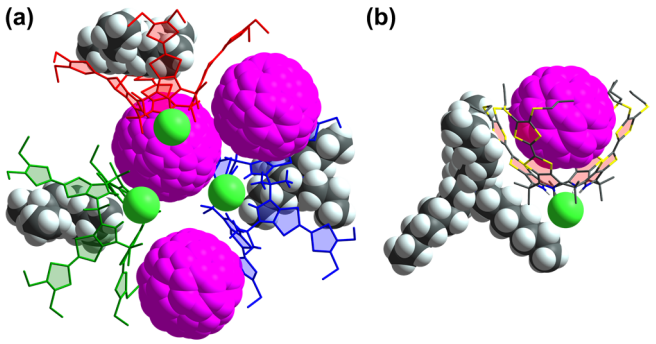

Fig. 7 Single-crystal X-ray structures of (a) **3** with TBACl and C_{60} and (b) **3** with TOACl and C_{60}.[42,43]

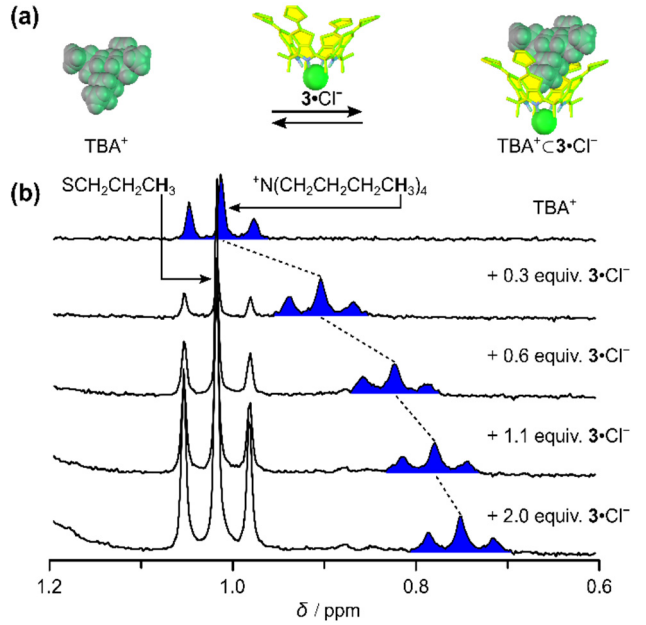

Fig. 8 Complexation of TBA^+ with **3**•Cl^-: (a) Scheme illustrating the complexation event and (b) partial ^1H NMR spectra ($CDCl_3$, 200 MHz) seen upon the addition of $TBAPF_6$ to a mixture of **3** and excess KCl containing six equiv. of dicyclohexano-18-crown-6, chemistry that generates **3**•Cl^- as the initial receptor-containing species. Adapted from Ref. 47. Copyright 2008, with permission from Elsevier.

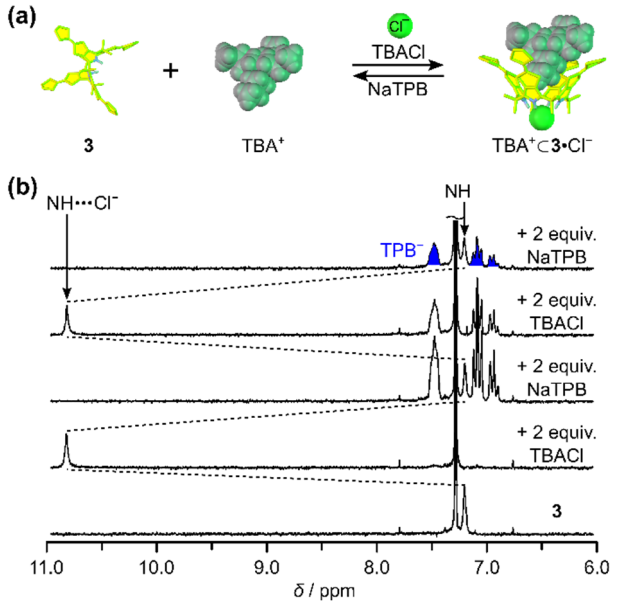

Fig. 9 Complexation of **3** and TBA^+ in the presence and absence of chloride anion: (a) Mechanistic scheme illustration the complexation event, (b) partial ^1H NMR spectra ($CDCl_3$, 200 MHz) of **3** upon stepwise addition of TBACl and NaTPB respectively, showing the complexation and decomplexation of chloride. Adapted from Ref. 47. Copyright 2008, with permission from Elsevier.

single crystal structural analysis of the tetraoctyl ammonium (TOA^+) chloride complex of **3** in the presence of C_{60} confirmed a 1:1 complex stoichiometry in the solid state (Fig. 7b). The structure revealed that the C_{60} resides in the cone of **3**•Cl^- and that the TOA^+ counter cation is not bound to the complex. Under certain conditions, higher-order complexes can be stabilised. Support for this latter suggestion came from the observation of a CT absorption band that increases upon mixing of **3** and C_{60} in the absence of any cone-inducing anions (Fig. 6c).

Transient absorption spectroscopic studies of C_{60}⊂**3**•Cl^- in CH_2Cl_2 via femtosecond flash photolysis (740 nm) revealed features corresponding to the one-electron-reduced fullerene radical anion ($C_{60}^{\bullet-}$) at 1080 nm[45] and the one-electron-oxidised TTF radical cation ($TTF^{\bullet+}$) at 400 nm.[46] First-order kinetic analysis of the transient spectra gave an electron-transfer rate of 10^{12} s^{-1} and a lifetime of 3.1 ps.[42]

In a subsequent study by Nielsen *et al*. the effect of the counter-cation on the complexation behaviour of **3**•Cl^- was probed. It was found that upon adding **3**•Cl^- to a $CDCl_3$ solution of TBA^+ (as its PF_6^- salt) the methyl proton resonances shifted upfield in the ^1H NMR spectrum. This was interpreted in terms of inclusion of TBA^+ into the cavity of **3**•Cl^- (Fig. 8). On the basis of a continuous variation Job plot, the complex stoichiometry was determined to be 1:1 for the binding of this specific cation to the pre-formed cone conformer giving TBA^+⊂**3**•Cl^- as the product. The corresponding association constant was estimated to $K_a = 7.4 \times 10^3$ M^{-1}.[47] This K_a value is two orders of magnitude lower than that obtained for the direct binding of TBACl to **3** as inferred from ITC ($K_a = 9.8 \times 10^5$ M^{-1}). In the same study, the interaction of tetraethylammonium (TEA^+) chloride with **3** was investigated by ITC. This gave a similar K_a value of 8.7×10^5 M^{-1}. This concordance was taken as evidence that these two tetraalkyl ammonium (TAA^+) cations do not affect the overall complexation behaviour. Two hypotheses were put forward to

Table 1 Complexation constants corresponding to the binding of anions by various symmetrical TTF-based calix[n]pyrroles

		TTF-C[4]P Binding constants [M^{-1}]						
		3	**5**	**6**	**7**	**8**	**10**	**11**
Binding ion (pair)	F^-	–	1.2×10^6 [a]	2.1×10^6 [b]	–	–	–	–
	Cl^-	7.8×10^5 [a] 1.5×10^7 [a,c] 1.8×10^5 [a,d] 1.9×10^4 [d,e] 2.5×10^6 [f]	5.2×10^5 [a] 2.3×10^7 [a,c] 1.7×10^4 [d,e]	1.2×10^5 [b]	1.2×10^5 [f] 2.9×10^3 [g]	6.6×10^5 [f] 4.3×10^4 [g]	1.3×10^4 [a]	5.3×10^6 [a]
	Br^-	3.0×10^4 [a,d] 5.8×10^4 [f] 6.0×10^4 [g]	2.1×10^4 [a]	7.6×10^3 [b]	2.2×10^3 [f] 9.6×10^1 [g]	8.3×10^3 [f] 5.3×10^2 [g]	8.3×10^3 [a]	3.4×10^4 [a]
	I^-	–	4.8×10^2 [a]	–	–	–	–	1.8×10^3 [a]
	AcO^-	1.3×10^6 [f]	1.4×10^5 [a]	–	6.5×10^4 [f]	3.9×10^5 [f]	2.2×10^4 [a]	8.7×10^5 [a]
	$H_2PO_4^-$	–	1.0×10^5 [a]	–	–	–	1.4×10^4 [a]	1.1×10^5 [a]
	HSO_4^-	–	1.4×10^2 [a]	–	–	–	2.7×10^3 [a]	1.1×10^5 [a]

[a] UV-Vis ($CHCl_3$). [b] ^1H NMR (CD_3CN w. 0.5% v/v D_2O). [c] TEA^+ as counter-cation. [d] THA^+ as counter-cation. [e] UV-Vis (PhCN). [f] ITC (CH_2ClCH_2Cl). [g] ^1H NMR (CD_2Cl_2).

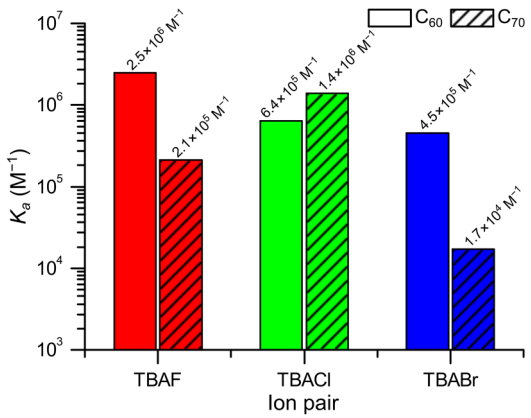

Fig. 10 Estimated binding constants of $TBA^+ \subset$**5**$\bullet X^-$ with fullerene based on a normal titration protocol.

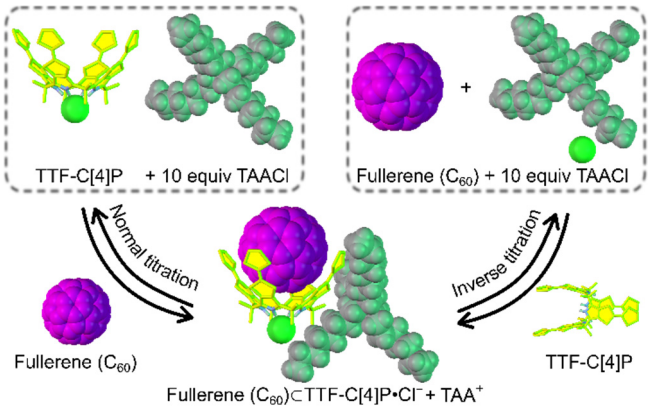

Fig. 11 Illustration of the two titration methods used to probe the interactions between TTFC[4]P and fullerene.

account for the similar binding strengths: (i) The relatively high affinity for anions could be masking the effect of the weaker cation/calix[4]pyrrole interaction or (ii) the electron-rich cavity formed from **3** as a result of anion complexation is large enough to encapsulate equally either the TEA^+ or the TBA^+ cation.[47] In the case of TBACl, switching of the formed $TBA^+ \subset$**3**$\bullet Cl^-$ cone complex to the presumed 1,3-alternate conformation was performed by adding sodium tetraphenylborate (NaTPB, Fig. 9). This addition serves to precipitate out NaCl and generate TBATPB, a species that does not complex well with **3**.[47]

In the study by Sessler[44] and co-workers noted above, the interactions between the TTF-C[4]Ps **3** and **5** and fullerenes C_{60} and C_{70} were studied under varying conditions and with different anions and counter-cations to determine the binding constants and the charge recombination dynamics of their CT complexes. Interestingly, variations in the halide anion could be exploited to alter the selectivity between C_{60} and C_{70} (Fig. 10). The choice of TAA^+ cation was also found to alter the binding affinity for C_{60}. In order to probe the relatively complex thermodynamics governing the interactions between these three key species, namely TTF-C[4]P, TBAX and fullerene, two complementary titration methods were applied. First, a normal titration (Fig. 11) of CH_2Cl_2 solutions of **5** with up to ten equiv. of TBAX was carried out in the presence of fullerene (C_{60} or C_{70}) to form complexes $TBA^+ \subset$**5**$\bullet X^-$ and $C_{60/70} \subset$**5**$\bullet X^-$, respectively. Second, an inverse titration (Fig. 11) was carried out wherein CH_2Cl_2 solutions containing fullerene (C_{60} or C_{70}) and ten equiv. of TBAX were titrated with **5**. Under these latter conditions the relative ratios of **5**, TBAX and fullerene vary. The fullerene binding constants derived from these two titrations differ for both fullerenes, as might be expected given the different competition effects at play. However, in terms of the influence of the halide anion on the binding of C_{60} there is a clear trend, namely $K_a(F^-) > K_a(Cl^-) > K_a(Br^-)$, a finding that correlates well with the basicity of the anions. In contrast, the complexation of C_{70} by **5** is subject to a different halide-dependency. In this case, TBACl produces the strongest complex as compared to both TBAF and TBABr. It was thus inferred that for a set of complexes in their cone conformations, the most optimal binding of C_{60} is seen with the fluoride anion, but with the chloride anion in the case of C_{70}. From control UV-Vis absorption spectroscopic titrations of **5** with various TBAX salts carried out in CH_2Cl_2 in the absence of a fullerene the following inherent anion selectivity was inferred: $K_a(F^-) > K_a(Cl^-) > K_a(Br^-)$. This study serves to illustrate how positive heterotopic allosteric modulation can be induced in a synthetic receptor via the choice of the halide anion "cofactor".

In the same study, Sessler and co-workers carried out a normal titration following the same protocol. Here, different TAA^+ chloride salts were tested for their effect on the complexation of C_{60} by **5**. The binding of C_{60} was found to depend on choice of ammonium cation. Specifically, tetrahexylammonium chloride (THACl) gave a binding constant of 2.3×10^6 M^{-1}, TBACl gave 6.4×10^5 M^{-1}, while the value with TEACl was 2.4×10^3 M^{-1}. These findings, taken in conjunction with the results of previous studies by Nielsen *et al.*[42,47] (Fig. 5, 7–8), provided further support for the notion that small electron-deficient TAA^+ cations are bound within the cavity of the cone conformer of TTF-C[4]P$\bullet Cl^-$ in accord with the following sequence: $TEA^+ > TBA^+ > THA^+$.

Femtosecond transient absorption spectroscopic studies of the supramolecular fullerene complexes of TTF-C[4]P **3** and **5** (studied using C_{60} and both C_{60} and C_{70}, respectively) with the three TBAX ($X^- = F^-$, Cl^- and Br^-) salts were carried out. In all cases, photoinduced electron transfer (PET) was observed instantaneously upon photoirradiation. This was interpreted in terms of a rapid electron transfer (ET) from the TTF units of the TTF-C[4]P receptor to the fullerene leading to formation of a charge separated (CS) state. Charge recombination (CR) dynamics of the various resulting ensembles was shown to occur with half-lives of 3.4–4.6 ps.[44] Such findings are consistent with the proposed fullerene$\subset$TTF-C[4]P$\bullet X^-$ complexes being formed in solution. Although the half-lives are similar, a correlation between the CR time constants and the various halides was found, with the half-lives increasing in the order of F^- (3.4–3.6 ps) < Cl^- (4.3–4.5 ps) ≤ Br^- (4.5–4.6 ps). This trend is in accord with the anion-induced structural variations of the complexes and highlights the need for the system to be stabilised as the cone conformer in order to encapsulate fullerene.

In summary, the judicial choice of both anion and accompanying TAA^+ cation can have a direct impact on the complexation behaviour of TTF-C[4]P as receptors for fullerenes.

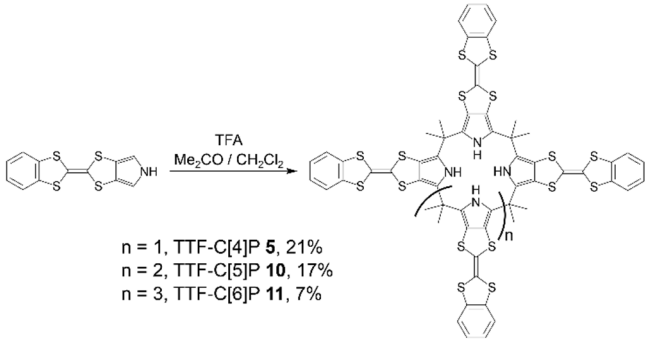

Scheme 1 Synthesis of TTF-C[n]P **5**, **10** and **11**.

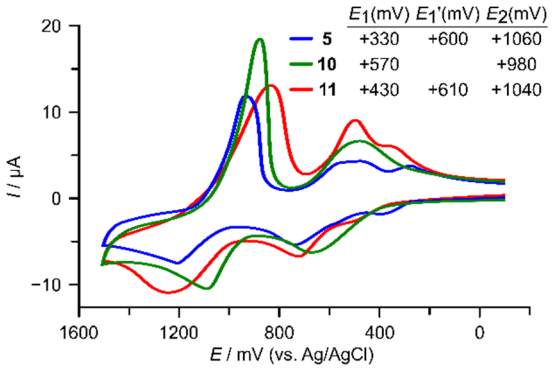

Fig. 12 Cyclic voltammograms of **5**, **10** and **11** (0.2 mM in $CHCl_3$) recorded at 100 mV s^{-1} (reference electrode, Ag/AgCl; supporting electrolyte, $TBAPF_6$ (0.4 mM)). Adapted from Ref. 48 with permission from The Royal Society of Chemistry.

Higher order tetrathiafulvalene-calix[*n*]pyrroles

In addition to the parent calix[4]pyrrole system, higher order calix[n]pyrroles have been synthesised and studied for their ability to complex anions and planar electron-deficient species (*e.g.* TNB and TNT).[48] The TTF-C[n]P species in question were prepared using the same protocol used to obtain the parent TTF-C[4]P system (Scheme 1). CV analyses of the three TTF-C[n]P congeners **5**, **10** and **11** in $CHCl_3$ (Fig. 12) provided the 2*n*-electron oxidation potentials where *n* refers to the number of TTFs in the C[*n*]P. The first oxidation event, which serves to generate the TTF radical cations (i.e. $(TTF^{\bullet+})_n$-C[n]P), is split into two separate waves for **5** and **11**, whereas in the case of **10** only a single wave is seen for this 5 × 1-electron oxidation step. This disparate behaviour was rationalised on the basis of the geometry of the three different macrocycles. Specifically, it was proposed that **5** and **11** are relatively flexible; this allows for opposing TTF subunits to approach to form stable mixed valence dimers $[(TTF)_2]^{\bullet+}$. In contrast, the C[5]P system is geometrically constrained such that there are no two TTF subunits directly opposite from one another.[48] The first oxidation waves thus follow the trend (Fig. 11) **5** < **10** < **11**. Standard UV-Vis absorption spectroscopic titrations were used to estimate the binding stoichiometries and complexation constants of the various TTF-C[n]Ps. On this basis, it was concluded that the parent TTF-C[4]P system **5** showed the strongest affinity for TNB and TNT (*vide infra*), while the TTF-C[6]P system **11** displayed the highest affinity for anions (*e.g.* chloride and acetate anions as their TBA^+ salts; see Table 1). The TTF-C[5]P system **10** proved least effective as a receptor for either class of substrates. Continuous variation Job plot analyses[42] of the interaction between TNB and **10** and **11**, respectively, proved consistent with a 1:1 binding stoichiometry in both cases. The corresponding binding constants were estimated to be 220 M^{-1} and 480 M^{-1}, respectively, based on the concentration-dependent increase in the CT absorption band intensity at λ = 650 nm. Analogous titrations with various TBA^+ anion salts were carried out for all three receptors in this series. In this case, the change in absorption at λ = 370 nm was monitored as a function of anion concentration. The resulting anion affinities followed the general trend TTF-C[6]P (**11**) > TTF-C[4]P (**5**) > TTF-C[5]P (**10**). An exception was seen in the case of $H_2SO_4^-$, where an affinity order of TTF-C[6]P (**11**) > TTF-C[5]P (**10**) > TTF-C[4]P) (**5**) was observed. Similar observations were made by Kohnke and co-workers in the case of β-free calix[n]pyrroles.[49]

Although it might be expected that the larger TTF-C[n]Ps would favour the binding of larger halide anions, this did not prove to be the case. Throughout the series **5**, **10** and **11** the relative binding affinity for halides followed the order Cl^- > Br^- > I^-. This was taken as an indication that the effects of charge density dominate over the putative benefits of size and shape complementarity, at least for this set of receptors and anions.

X-ray diffraction based solid-state structures revealed that the chloride anion is bound to TTF-C[4]P **5** and TTF-C[5]P **10** with

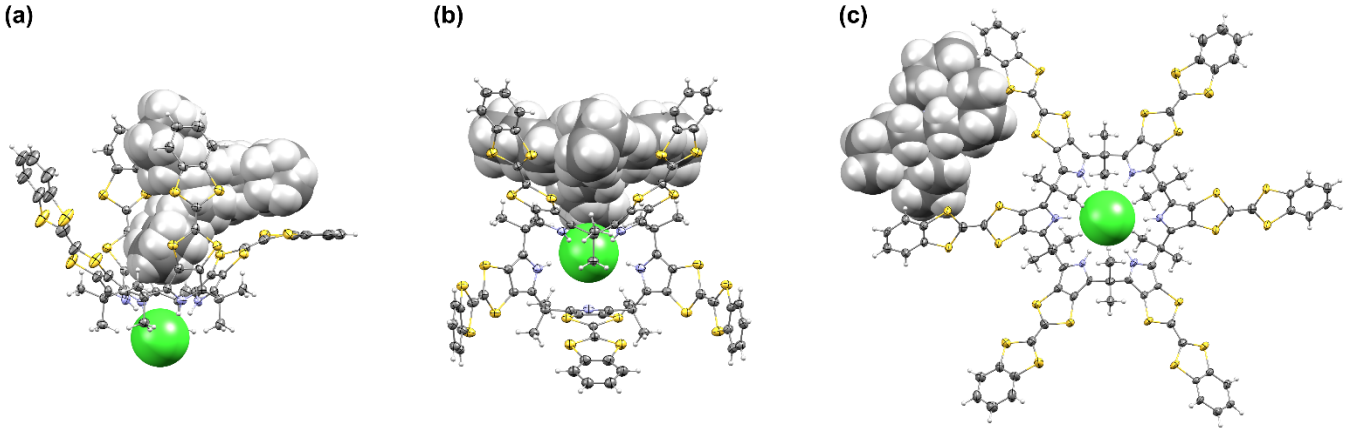

Fig. 13 Single-crystal X-ray structure of the complexes of (a) **5** with TBACl, (b) **10** with THACl and (c) **11** with TBACl. Thermal ellipsoids are scaled at the 30% probability level.[48]

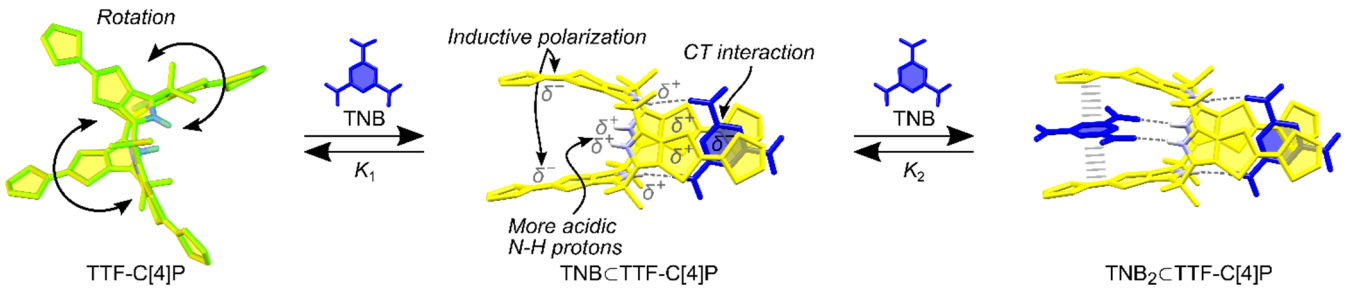

Fig. 15 Schematic representation of the electronically induced effects of TTF-C[4]P that occur upon binding a single electron-deficient planar guest (*e.g.* TNB). This first recognition event results in a formation of preferentially organised 1,3-alternate conformation. It also increases the acidity of the free (*i.e.* uncomplexed) NH protons and enhances the electron density of the uncomplexed TTF-C[4]Ps. These effects lead to a cooperative binding mode where $K_2 >> K_1$.[41,50]

the receptor in the cone conformation. In contrast, TTF-C[6]P **11** adopts a planar geometry with the chloride perfectly situated within the centre of the macrocycle. In the case of TTF-C[5]P **10**, the cone conformation shows a high degree of distortion and only four of the five NH protons are seen to be in close proximity to the chloride anion.

Improved binding of explosives

Following the initial report of TTF-C[4]P **3** being able to complex two molecules of TNB and producing a colourimetric response, follow up studies were initiated by Sessler and Jeppesen. Here, key goals were to (i) improve the sensitivity for nitroaromatic guests by increasing the inherent binding interactions and (ii) decrease the affinity for anions. Efforts were also made to lock the receptor in the 1,3-alternate conformation.

In 2010, Sessler and co-workers detailed the synthesis of two π-extended TTF-C[4]Ps wherein the terminal 1,3-dithiole moiety was annulated with either thiophene (**4**) or benzene (**5**) (Scheme 1).[50] As compared to the earlier TTF-C[4]P system **3**, these new TTF-bearing calix[4]pyrroles are more rigid, less soluble and characterised by greater access to the binding sites in the 1,3-alternate conformation (*i.e.* reduced steric hindrance). A crystal structure of the complex formed between **5** and picric acid (TNP) (Fig. 14) provides support for these contentions. On the other hand, CV measurements revealed that the π-extended systems were weaker electron donors with first half-wave oxidation potentials of $E^1_{½}$ =0.29 V, $E^1_{½}$ =0.37 V, and $E^1_{½}$ =0.30 V for **3**, **4** and **5** , respectively. On this basis, the higher TNB affinities recorded for **4** and **5** *vs*. **3** (Table 2) were thought to reflect a decrease in steric hindrance effects, rather than an improvement in electronics *per se*. Factors such as solubility may also play a role.

The recognition of nitroaromatic guests by these TTF-C[4]Ps receptors was found to be subject to positive homotropic allosteric binding (Fig. 15). It was considered likely that the TTF-C[4]Ps **3**–**5** would be partly preorganised for binding of electron-deficient aromatic planar guests in their respective 1,3-alternate conformations. However, the dynamic nature of the receptor, having free rotation around the σ-bonds in the C[4]P core were nevertheless expected to preclude full preorganisation of the receptor. Therefore, the first binding event was expected to impact the second binding event by creating a more rigid and suitable binding environment. Electronic and pyrrole NH hydrogen bond donor effects were also expected to be enhanced (Fig. 15). Specifically, it is noted that binding of the first electron deficient substrate occurs via a combination of CT and hydrogen bonding interactions. This results in a polarisation of the TTFs in the vacant binding site making them more susceptible to CT interactions with a second substrate. This polarisation also makes the remaining pyrrole NH protons more acidic, thus enhancing their ability to hydrogen bond to the nitro groups present in the second nitroaromatic substrate. This results in cooperative binding.

The binding of oxygen to haemoglobin provides a paradigm for positive cooperative effects.[51,52] The classic Adair[53] and Hill[54]

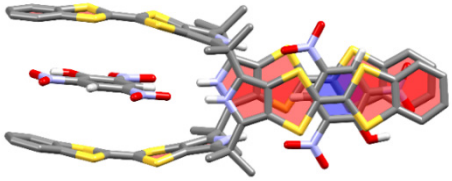

Fig. 14 Single-crystal X-ray structure of the TNP_2⊂**5** complex. All hydrogen atoms except the NH and Ar-H protons have been removed for clarity.[50]

Table 2. Complexation constants and Hill parameters (*n*) for the binding of electron-deficient aromatic guests with the TTF-based calix[4]pyrroles **3**–**5** based on UV–Vis absorption spectroscopic titrations of the receptors (0.2 mM in $CHCl_3$) fitted with the Hill[54] and Adair[53] equations. Estimated errors are ≤ 12%[50]

Complex	K_a [M^{-2}]	*n*	K_1 [M^{-1}]	K_2 [M^{-1}]
TNB_2⊂**3**	4.3×10^3	1.27	3.9×10^2	1.4×10^3
TNP_2⊂**3**	3.8×10^3	1.30	2.8×10^2	1.2×10^3
TNT_2⊂**3**	3.3×10^2	1.23	5.9×10^1	2.0×10^3
TNB_2⊂**4**	3.4×10^6	1.70	1.3×10^3	3.1×10^4
TNP_2⊂**4**	3.7×10^6	1.86	6.4×10^2	2.0×10^4
TNT_2⊂**4**	2.3×10^4	1.45	3.2×10^2	2.8×10^3
TNB_2⊂**5**	1.5×10^5	1.34	2.8×10^3	1.7×10^4
TNP_2⊂**5**	9.1×10^4	1.34	1.7×10^3	1.1×10^4
TNT_2⊂**5**	1.2×10^4	1.31	5.7×10^2	2.6×10^3

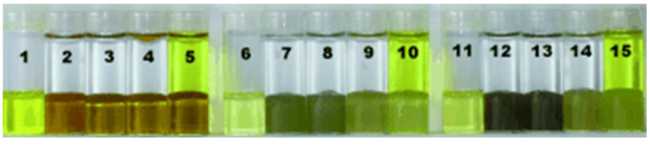

Fig. 16 Colourimetric sensing of TNB, TNT and TNP using receptors **3**–**5** (2 mL of 0.2 mM in $CHCl_3$) and test nitroaromatic explosives TNB, TNT and TNP (3 mL of 0.2 mM in H_2O) in the absence and presence of salts (2 mM of $NaHCO_3$, K_2CO_3, $MgSO_4$, $CaCl_2$ and NH_4Cl each). Vials from the left contain: 1) **3**, 2) **3** + TNB, 3) **3** + TNB + salts, 4) **3** + TNT, 5) **3** + TNP, 6) **4**, 7) **4** + TNB, 8) **4** + TNB + salts, 9) **4** + TNT, 10) **4** + TNP, 11) **5**, 12) **5** + TNB, 13) **5** + TNB + salts, 14) **5** + TNT and 15) **5** + TNP. Reprinted from Ref. 50. Copyright 2010 Wiley-VCH Verlag GmbH.

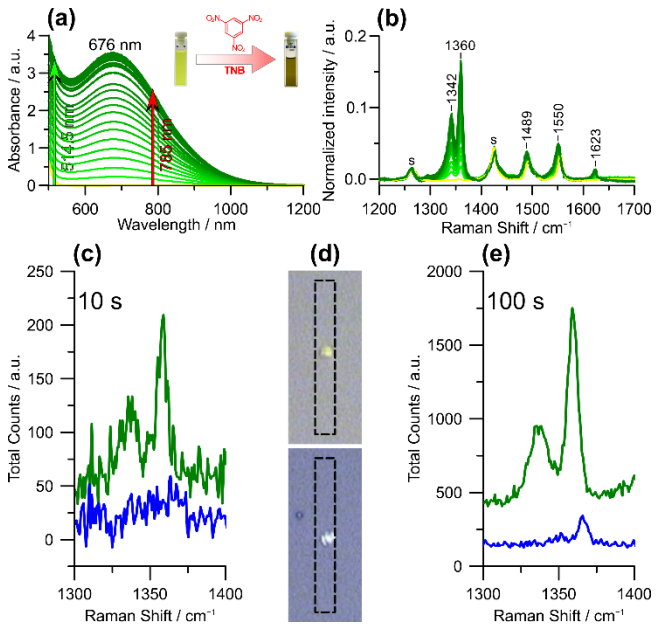

Fig. 17 Solution and solid-state detection of TNB by **3**. (a) UV-Vis-NIR absorption spectroscopic titration of **3** (30 mM in CH_2Cl_2 at 298 K) with TNB (0–6 equiv.). (b) Resonance Raman spectra of the same titration with excitation at λ = 785 nm. (c) and (e) Solid-state resonance Raman spectra (λ_{exc} = 785 nm) of microcrystalline samples of **3** ((d) top, blue line) and TNB_2⊂**3** ((d) bottom, green line) subject to laser photoexcitation (0.3 mW) for 10 and 100 s, respectively. Adapted from Ref. 57 with permission from The Royal Society of Chemistry.

equations for cooperative binding were thus applied to this set of TTF-C[4]P receptors. Based on UV-Vis absorption spectroscopic titrations of receptors **3**–**5** with the electron-deficient guests TNB, TNT and TNP, binding constants (K_1 and K_2) for each recognition event, the overall binding affinity (K_a), and the Hill coefficient (n) were estimated (Table 2). All three receptors showed cooperative binding with Hill coefficients, n > 1.[§] TTF-C[4]P **4** displayed the strongest degree of cooperativity with n = 1.86 for the binding of TNP. The general trend in binding strength of neutral planar guests for the three receptors proved to be **3** < **4** < **5**, with **4** and **5** binding most substrates two to three orders of magnitude more effectively than **3**.

To test the receptors as colourimetric sensors for nitroaromatic explosives in the presence of salts, solutions of the receptors were mixed with aqueous solutions of the target nitroaromatic substrates. This resulted in an immediate colour change from yellow to green. To determine the anion sensitivity, a mixture of $NaHCO_3$, K_2CO_3, $MgSO_4$, $CaCl_2$ and NH_4Cl salts (2 mM each) were included in the aqueous TNB solution. Photos of the different mixtures are shown in Fig. 16. In general, all of the samples containing the nitroaromatic substrates in the salt mixture were characterised by a greenish colour.

Actual devices were prepared by using a micro-cantilever setup. Two separate studies were reported. Both allowed for detection at low concentration limits.[55,56] These studies relied on the change in mass of the receptor upon binding explosives producing a change in reflection of the cantilever yielding gas phase detection limits of 10 ppb[55] in the case of **4** and TNB, as well as <10 ppm[56] in the case of **3** and 2,4-dinitrotoluene (DNT). Another example of enhancing sensitivity was reported by Flood and co-workers.[57] They succeeded in detecting nitroaromatic explosives by monitoring the resonance Raman features of the CT band of the complex produced upon mixing receptor **3** with a nitroaromatic analyte (*i.e.* TNB).[57] Using this platform and a laser excitation wavelength of λ = 785 nm, two Raman-active nitro bands at 1360 and 1342 cm^{-1} were observed (Fig. 17b). A factor 14–20 increase in signal strength was observed for the complex. Crystals of pure **3** and TNB_2⊂**3** (Fig. 17c–e) could also be analysed in this way.

The intricate process of positive homotropic allosteric binding provides insight into possible avenues for improving the ability of TTF-C[4]Ps to act as sensors for nitroaromatic explosives (e.g. TNT and TNB). However, at the present time studies in solution are inconclusive as to which interactions are decisive. Conversely, solid state devices for gas phase detection do not show large differences in detection limits, thus leading to the inference that π-surface interactions, steric hindrance, and solubility considerations do not play critical roles in mediating the observed sensing effects.

Modified TTF-C[4]Ps for sensing applications

It was assumed that if the anion-binding interactions were relatively repressed, the TTF-C[4]P scaffold could be enhanced as a sensor for electron deficient guests. Several efforts have thus been made to reduce the number of available NH hydrogen bond donors within the C[4]P framework. In this context, Poulsen *et al.*[58] reported a bis(TTF)-calix[2]pyrrole-[2]thiophene **12** in 2007 (Fig. 18). It was expected that this system would adopt a 1,3-alternate conformation wherein the binding pocket between the two TTF units lacks donating NH protons. It was thus expected that complexation with electron-deficient guests would be driven almost exclusively via CT interactions. In fact, receptor **12** was found to complex 7,7,8,8-

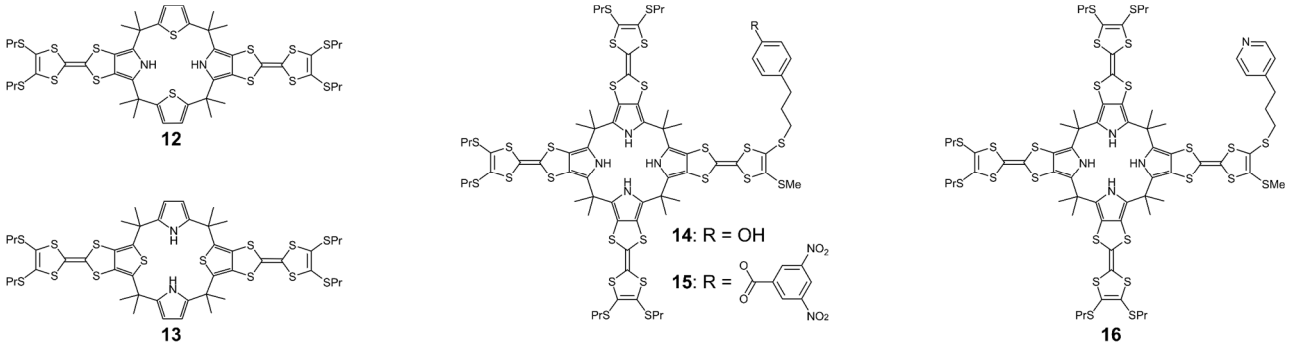

Fig. 18 Chemical structures of modified TTF-C[4]Ps **12**–**16**.

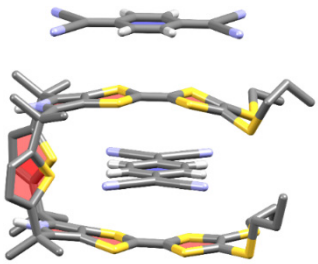

Fig. 19 Single-crystal X-ray structure of the complex TCNQ⊂**12**•TCNQ obtained by slow evaporation of a CH_2Cl_2 solution of equimolar concentration of **12** and TCNQ. CH_2Cl_2 and CH hydrogen atoms on **12** have been removed for clarity.[58]

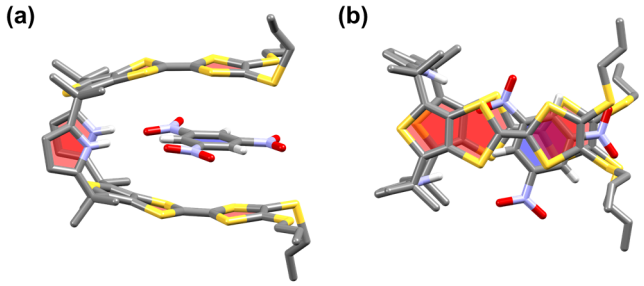

Fig. 20 Single-crystal X-ray structure of the complex TNB⊂**13** obtained by slow diffusion of *n*-hexane into a CH_2Cl_2 solution containing an equimolar mixture of **13** and TNB. The structure is shown in side (a) and top (b) views. The CH hydrogen atoms on **13** have been removed for clarity.[59]

tetracyanoquinodimethane (TCNQ) in its 1,3-alternate conformation. Single crystal X-ray analysis (Fig. 19) revealed the inclusion of a TCNQ guest between the TTF units with the pyrrole NH protons facing away from the bound substrate. Another TNCQ molecule was found to reside on the outside of one of the TTF units of **12**. The average distance between the TTF units and the planar TCNQ was consistent with the formation of a CT complex.[40] Further support for complex formation came from absorption spectral studies of a 1:1 mixture of **12** and TCNQ. The resulting spectrum was characterised by the presence of CT absorption bands with maxima at λ = 749 and 851 nm that were not seen in the individual components. Electron paramagnetic resonance (EPR) measurements involving similar mixtures revealed the presence of a weak radical signal centered at g = 2.010 that was ascribed to the presence of a TTF radical cation and a TCNQ radical anion.

In the quest to prepare an anion-insensitive TTF-C[4]P receptor, Kim *et al*. prepared the isomeric system (**13**; Fig. 18)

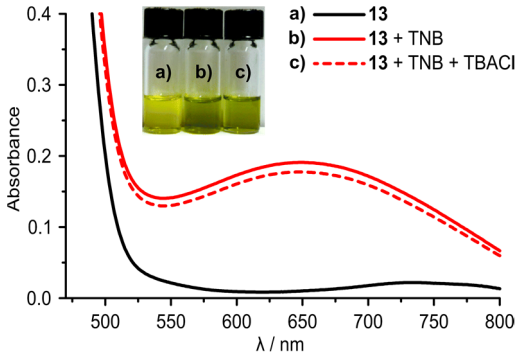

Fig. 21 UV-Vis absorption spectroscopic titration (CH_3Cl, 298 K) of **13** with addition of five equiv. of TNB and subsequent addition of ten equiv. of TBACl. Insert of the solutions during titration. Adapted with permission from Ref. 59. Copyright 2009 Springer.

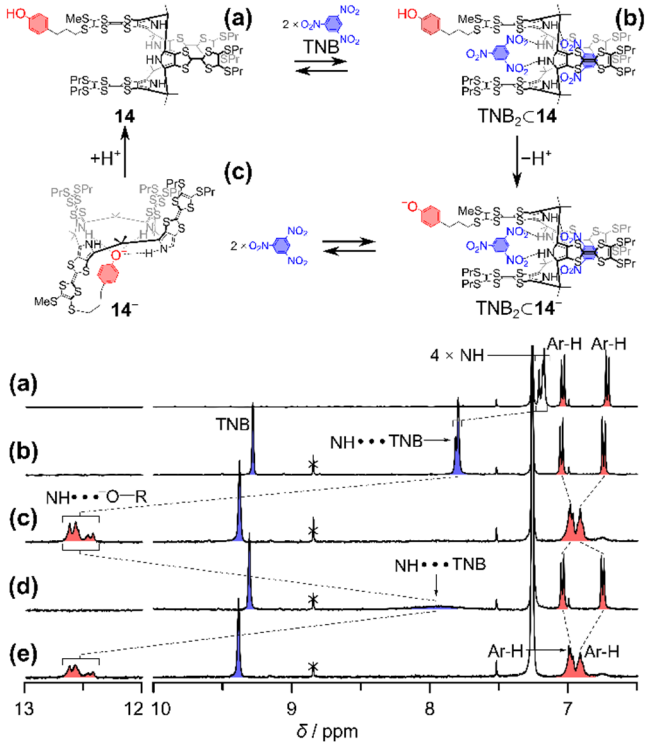

Fig. 22 Schematic illustration (top) of the molecular recognition events that are seen for **14** with TNB in the presence of acid and base and partial ^{1}H NMR spectra (400 MHz, 298 K, $CDCl_3$) of (a) receptor **14** (1.5 mM), (b) **14** + two equiv. TNB, (c) **14** + two equiv. TNB + one equiv. DBU, (d) **14** + two equiv. TNB + one equiv. DBU + one equiv. MSA and (e) **14** + two equiv. TNB + one equiv. DBU + one equiv. MSA + one equiv. DBU. Adapted from Ref. 60. Copyright 2011 Wiley-VCH Verlag GmbH.

where the TTF units are likewise appended to thiophene moieties.[59] A comparison of **12** and **13** by electrochemical methods revealed some significant differences. For instance, **12** displays a first two-electron oxidation wave at $E_{½}^1$ = +0.075 V (vs. Fc^+/Fc), while oxidation of **13** proceeds via two one-electron processes characterised by $E_{½}^1$ values of –0.067 V and +0.90 V, respectively (vs. Fc^+/Fc). This electrochemical separation was taken as evidence of an electronic through-space communication between the two TTF units of **13**. In marked contrast to what was seen for the TCNQ complex of **12**, favourable hydrogen bonding interactions between the pyrrole NH protons of **13** and a bound TNB guest were observed in the solid state (Fig. 20).[59] As seen in the case of several other all-pyrrole TTF-C4Ps, the associated favourable interactions led to a colourimetric response that was observable to the naked eye (Fig. 21). ^{1}H NMR spectroscopic studies of the interactions between receptor **13** and TNB, TNP and TNT revealed shifts in the pyrrole NH proton resonances consistent with binding. The corresponding binding constants were estimated to be K_a = 3 M^{-1}, 6 M^{-1} and <1 M^{-1} for TNB, TNP and TNT, respectively. The interactions with TBACl proved too weak to be monitored by ^{1}H NMR spectroscopy.

The modified TTF-C[4]P receptors **12** and **13** are examples of the significance of having both hydrogen bonding and CT interactions when complexing nitroaromatic guests. Furthermore, the lack of preorganisation in these receptors highlight the significant cooperative binding effect that are

central in the tetra-TTF-C[4]P's **3**–**5**. Thus, retaining that core structure with four TTF units appears essential.

A complex TTF-C[4]P receptor with three thiopropyl-substituted TTFs and one TTF bearing a phenol moiety **14** (Fig. 18) was reported by Nielsen *et al.*[60] In the case of **14** the NH proton resonances in the ^{1}H NMR spectrum ($CDCl_3$) are separated into three singlet signals that resonate at δ = 7.21, 7.19 and 7.18 ppm (Fig. 22a). It was expected that the presence of the phenolic moiety would allow for external control over the conformation of **14** in analogy to the work of Trauner and co-workers.[65] In fact, the addition of one equiv. of base (1,8-diazabicyclo-[5.4.0]undec-7-ene (DBU)) led to deprotonation of the phenol, which was found to trigger an allosteric change in the conformation of **14** from the initial 1,3-alternate conformation to a partial cone conformation in the case of **14**$^-$ (Fig. 22c). This latter species is presumably stabilised as the result of intramolecular anion-C[4]P binding. Adding one equiv. of methanesulfonic acid (MSA) served to regenerate the 1,3-alternate conformation of **14**. To estimate the strength of the intramolecular association, the interactions between **14** and TBACl were first assessed. Standard UV-Vis absorption spectroscopic titrations revealed a binding constant of K_a = 1.9 × 10^6 M^{-1}. The competition between **14**$^-$ and TBACl was then studied by ^{1}H NMR spectroscopy. The NH proton resonances of **14**$^-$ were found to split into two distinct signals, corresponding to self-complexation and chloride-complexation, as TBACl was added. This allowed a relative complexation constant, K_{rel}, of 1.5 to be determined. Combining these values, a K_a = 1.5 × 10^6 could be calculated for the intramolecular interaction within **14**$^-$.[62]

The controlled recognition of nitroaromatic explosives was demonstrated by means of a ^{1}H NMR spectroscopic titration (Fig. 22). When **14** was titrated with two equiv. of TNB, the four non-equivalent NH protons of **14** shift to lower field (*i.e.* from δ = 7.21, 7.19 and 7.18 ppm to δ = 7.82 and 7.80 ppm). This change was taken as evidence of intermolecular hydrogen bonding between **14** and the two bound TNB guests (Fig. 23b). In the resulting complex, TNB_2⊂**14**, the TNB CH protons are found to resonate at δ = 9.28 ppm. Addition of one equiv. of base (DBU) to a $CDCl_3$ solution of the TNB_2⊂**14** complex leads to a downfield shift in the TNB proton resonances and the emergence of a signal at δ = 9.37 ppm for the unbound TNB. Under these conditions, the NH protons of **14** shift to lower field (δ = 12.64–12.40 ppm) as would be expected for an intramolecular complexation event where the phenolate moiety participates in hydrogen bonding interactions with the NH protons (Fig. 23c). Re-protonation of **14**$^-$ via the addition of one equiv. of MSA was found to regenerate the TNB_2⊂**14** complex as confirmed by ^{1}H NMR analyses (Fig. 22d).

Nielsen *et al*. was able to convert **14** to the corresponding 3,5-dinitrobenzoate (DNB) ester **15** (Fig. 19).[63] This DNB-bearing TTF-C[4]P **15** proved incapable of forming a stable intramolecular complex, presumably because of the rigidity of the phenol-DNB ester (Fig. 23b). Instead, it undergoes dimerisation to form **15•15**. By monitoring the pyrrole NH, phenol OH and DNB proton resonances by ^{1}H NMR spectroscopy while diluting samples of **15** (Fig. 23b) the dimerisation constant could be estimated as K_1 = 1950 M^{-1}.

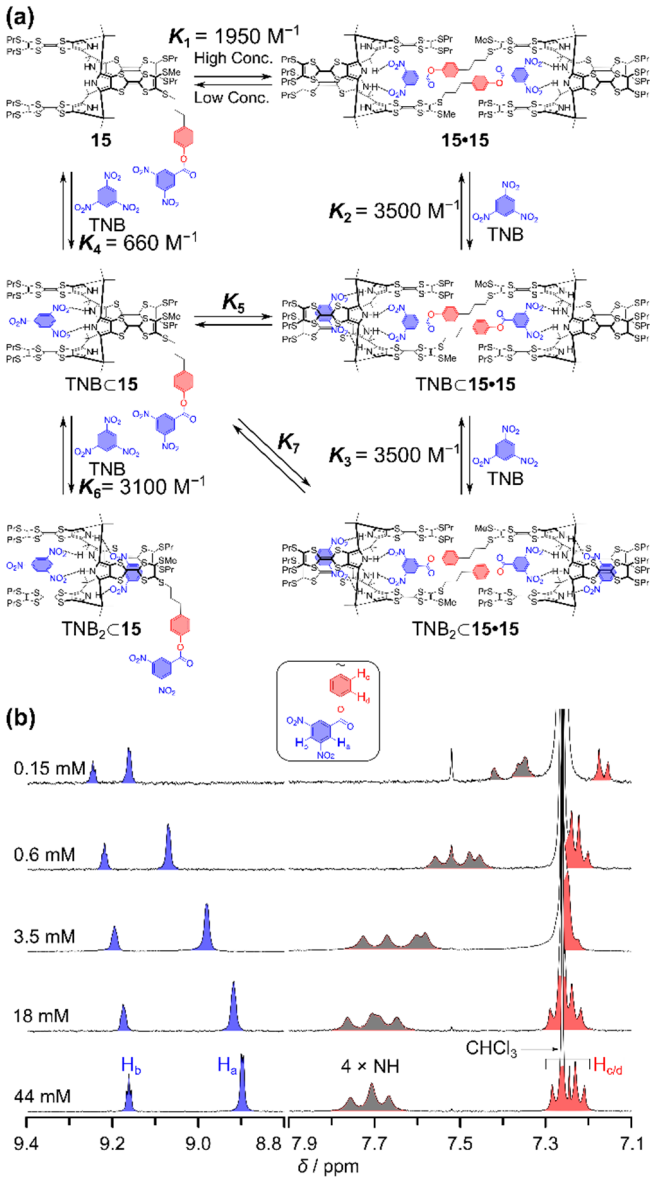

Fig. 23 Schematic overview (a) of the equilibria governing the complexation of TNB by **15**. The dimerisation constant (K_1) was derived from concentration-dependent ^{1}H NMR spectroscopic analyses (b) of solutions of **15** (0.15 mM to 44 mM recorded at 400 MHz in $CDCl_3$ at 298 K). The remaining equilibrium constants were estimated based on two ^{1}H NMR spectroscopic titrations of **15** (0.78 mM and 1.5 mM, respectively in $CDCl_3$ at 298 K) with increasing amounts of TNB. Adapted with permission from Ref. 63. Copyright 2011 American Chemical Society.

In CH_2Cl_2 solution, complex **15•15** is characterised by an absorption band centred at λ = 560 nm (Fig. 24a). Upon addition of TNB, an increase in spectral intensity is seen, along with a bathochromic shift in the absorption maximum to λ = 633 nm.[63] The dimerisation of **15** is thought to lead to a higher degree of preorganisation which was expected to favour the subsequent complexation of TNB. As shown in Fig. 23a, the equilibria become complex when TNB is introduced to solutions containing **15•15**. By analysing the proton resonances associated with the pyrrole NH and DNB H_a signals via ^{1}H NMR spectroscopy when solutions of **15** were titrated with increasing quantities of TNB, it proved possible to estimate the remaining equilibrium constants presented in Fig. 23a. The calculated values proved in good agreement with what might be expected

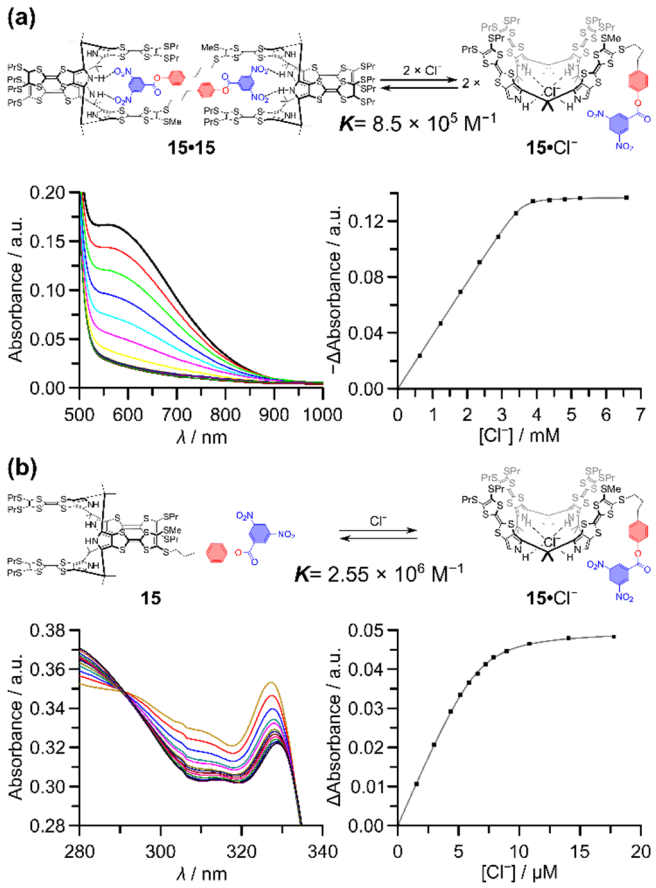

Fig. 24 UV-Vis-NIR absorption spectroscopic titrations (CH_2Cl_2, 298 K) of **15** with TBACl carried out at two different concentrations of **15**: (a) At high concentration (0.4 mM) the dimer **15•15** is a dominant species. (b) At low concentration (6.6 μM) the monomer **15** is the predominant species in solution, resulting in a higher apparent complexation constant for chloride anion binding. Adapted from Ref. 64. Copyright 2012, with permission from Elsevier.

for a preorganised system, with values of 3500 M^{-1} being noted for binding both the first and second TNB guest to **15•15**. In contrast, the first TNB guest binds relatively weakly to free **15**; however, the affinity for the second guest mirrors what is seen in the case of dimer **15•15**.

The inherent green colour of **15** in solution allowed the system to tested as a colourimetric sensor for anions.[64] Due to the dimeric nature of **15**, the green CT band attributed to interactions between TTF and DNB, was reduced upon addition of TBACl. The associated breakup in the intermolecular CT complex results in a colour change from green to yellow. Absorption spectral titrations of TBACl into a solution of **15** were used to monitor the associated spectral changes. When the titration was performed at a low concentrations of **15** the uncomplexed monomer **15** is present in significant quantities and able to complex chloride in its cone conformation; this was reflected in a change in the absorbance intensity at λ = 326 nm (Fig. 24b). A similar titration carried out at higher concentration revealed a lower K_a value for chloride anion complexation (Fig. 24a). This was interpreted in terms of receptor **15** being organised in a dimer-induced 1,3-alternate conformation at higher concentrations, reducing its inherent ability to complex the chloride anion.

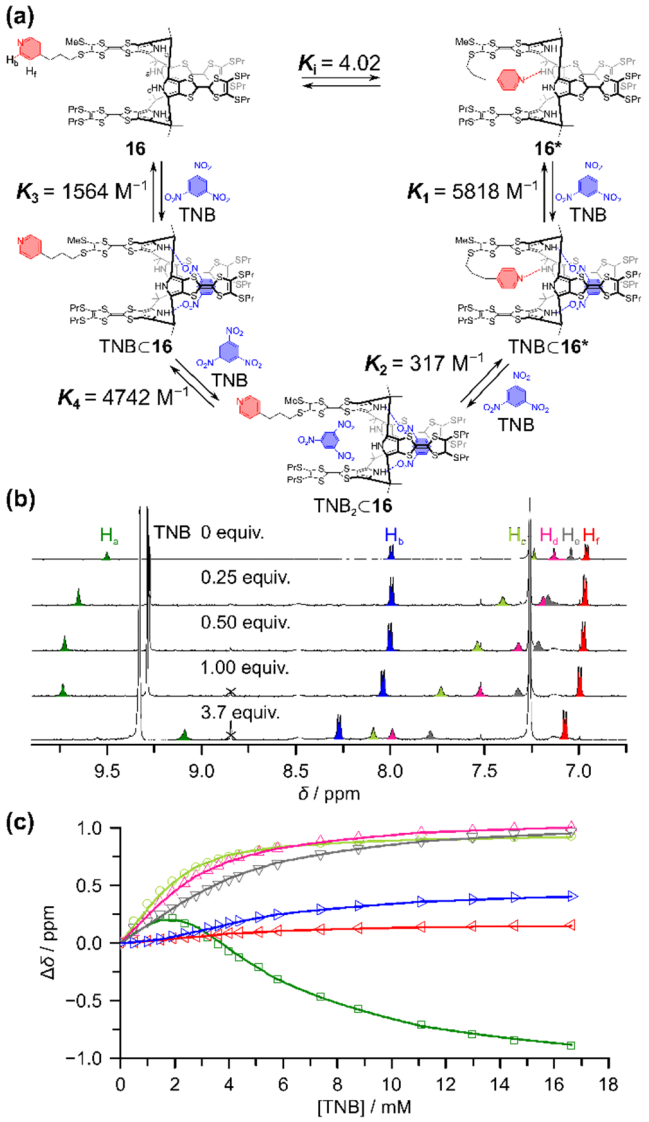

Fig. 25 Interactions of **16** and TNB shown in the form of (a) a mechanistic scheme with associated equilibrium constants as estimated by (b) ^{1}H NMR spectroscopic (400 MHz, 298 K, $CDCl_3$) titrations of **16*** (2.00 mM) with increasing quantities of TNB (0 to 8.3 equiv.) wherein the change in the chemical shift of the aromatic signals (c) related to four pyrrole NH protons and two pyridine proton resonances (symbols) are monitored. The lines indicate best fits to the binding isotherms. Adapted from Ref. 65. Copyright 2013 Wiley-VCH Verlag GmbH.

In an effort to increase the sensitivity of TTF-C[4]P receptors towards nitroaromatic explosives (e.g. TNB) Bähring *et al.* prepared the preorganised receptor **16** bearing one pyridine moiety (Fig. 18).[65] A ^{1}H NMR spectral analysis (Fig. 25b) revealed four distinct pyrrole NH signals resonating as singlets at δ = 7.04, 7.13, 7.24, and 9.50 ppm. Compared to **3**, the signal at δ = 9.50 ppm is shifted downfield by $\Delta\delta$ = 2.36 ppm. Dilution studies monitored by ^{1}H NMR spectroscopy as well as 2D NOESY NMR provided support for the presence of intramolecular hydrogen bonding interactions between the internal NH donor and pyridine hydrogen bond acceptor giving rise to a species referred to as **16***.

When receptor **16*** was titrated with TNB (0 to 1 equiv., Fig. 25b), the four NH proton signals shift to lower field. However, when the amount of TNB is increased (from 1 to 8.3 equiv.) the NH proton resonances shift upfield (Fig. 25b). These findings

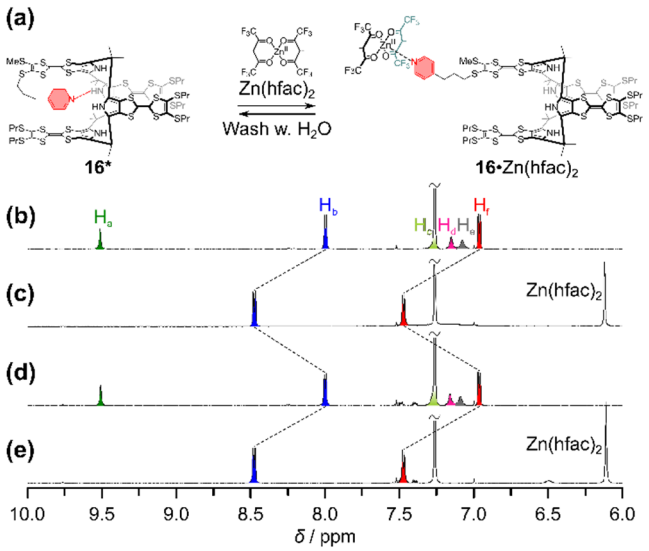

Fig. 26 Conformational control of receptor **16** by achieved by adding $Zn(hfac)_2$ and subjecting to an aqueous wash (a). Partial ^1H NMR spectra (400 MHz, 298 K, $CDCl_3$) of (a) **16** (1.0 mM), (b) **16** + $Zn(hfac)_2$ (one equiv.), (c) after washing the solution in (b) with H_2O and (e) after addition of $Zn(hfac)_2$ (one equiv.) to the solution in (d). Adapted from Ref. 65. Copyright 2013 Wiley-VCH Verlag GmbH.

provide support for the suggestion that **16*** is preorganised in the 1,3-alternate conformation and that there is a competition between the intramolecular interaction with the tethered pyridine and the TNB guest as shown schematically in Fig. 25a. The equilibrium constant K_i for the intramolecular complexation event was estimated to 4.0. This value, indicative of a weak complexation event, was supported by a reference ^1H NMR spectroscopic titration experiment wherein **3** was titrated with 4-methylpyridine (0–200 equiv.) for which an overall binding of K_a = 1.44 M^{-2} was derived.[65] However, the preorganisation of **16*** results in a large complexation constant for the first binding of TNB (K_1 = 5818 M^{-1}) and a small complexation constant for binding the second TNB guest (K_2 = 317 M^{-1}).

To preclude the preorganisation of **16***, a Zn(II) hexafluoroacetylacetonate complex ($Zn(hfac)_2$) capable of complexing the pyridine moiety was introduced. The interaction between the pyridine moiety and the zinc complex was exceptionally strong (outside the range of ^1H NMR spectral analysis).[66] When $Zn(hfac)_2$ was added to a solution of **16*** in $CDCl_3$, the proton resonances associated with the pyridine moiety were shifted downfield (Fig. 26c) and the four NH proton signals disappeared. These spectral changes were ascribed to receptor **16*** being converted into the corresponding complex **16**•$Zn(hfac)_2$, a species lacking any particular preorganisation (Fig. 26a). Aqueous extraction of $Zn(hfac)_2$ from the $CDCl_3$ allowed the receptor to return to the preorganised form **16*** (Fig. 26d). A ^1H NMR spectroscopic study of a $CDCl_3$ solution of **16**•$Zn(hfac)_2$ (2.00 mM in **16** + one molar equiv. of $Zn(hfac)_2$) revealed a broad singlet at $\delta \approx 7.1$ ppm attributed to the four NH protons. Upon treating with increasing quantities of TNB, this signal was seen to shift to lower field and become less broad. Upon the addition of ten equiv. of TNB, the NH proton signals were found to resonate as a triplet at δ = 8.14 ppm. These concentration dependent chemical shifts allowed binding constants of K_1 = 20 M^{-1} and K_2 = 1.2 × 10^4 M^{-1} to be estimated

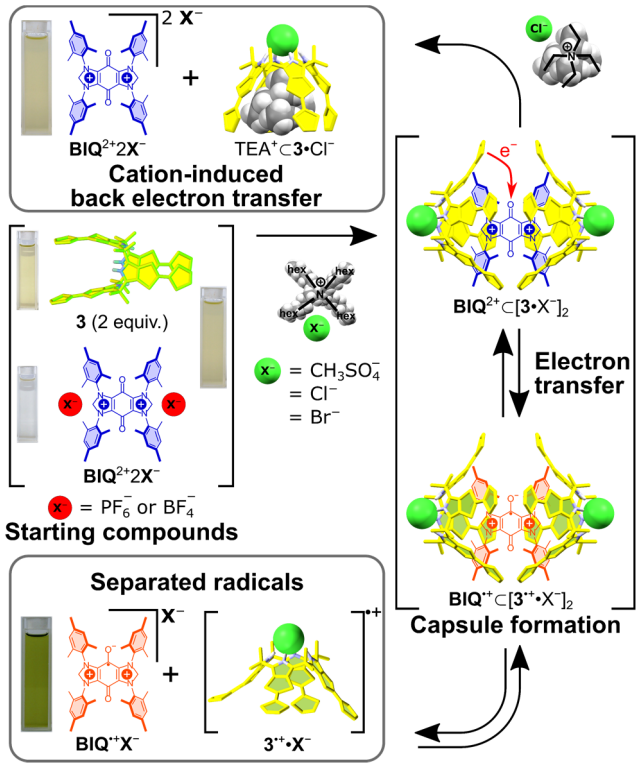

Fig. 27 Chemical structures of BIQ^{2+} and its radical form along with the proposed dynamical ion-mediated ET process of **3** and BIQ^{2+} upon introducing the appropriate stimuli in the form of anions and cations and controlled BET. Adapted from Ref. 67. Reprinted with permission from AAAS.

for the complexation of TNB. These values were taken as evidence of strongly positive cooperative binding.

Based on the above findings, we conclude that peripheral functionalisation of the core TTF-C[4]P receptor unit allows for the design of more intricate supramolecular systems that illustrate the subtle interplay between conformational control and complexation of ions in the recognition of electron deficient aromatic guests.

Electroactive and stimuli-responsive systems

Studies of **3** with a variety of ions, ion-pairs and neutral guests[35,39,42,44,47] revealed its ability to form a capsule-like binding pocket for electron-deficient guests in the presence of strongly bound anions. Anion recognition was also found to lower the first electron reduction potential which led to the suggestion that TTF-C4Ps could function as electroactive receptors whose recognition features could be fine-tuned by using ion-pairs as an external stimulus.

In 2010, Sessler and co-workers reported an ion-mediated ET event within a supramolecular donor-acceptor assembly consisting of the anion-bound form of TTF-C[4]P **3** and a dicationic bisimidizolium quinone (BIQ^{2+}, Fig. 27).[67] When **3** and BIQ^{2+} (with PF_6^- or BF_4^- as the counter anion) are mixed together in $CHCl_3$, no apparent interactions are seen. This is rationalised as **3** retaining the 1,3-alternate conformation that is unable to interact strongly with the large BIQ^{2+} guest. However, addition of an ion-pair containing THA^+ as the cation and either $CH_3SO_4^-$, Cl^-, or Br^- as the anion, induces conversion

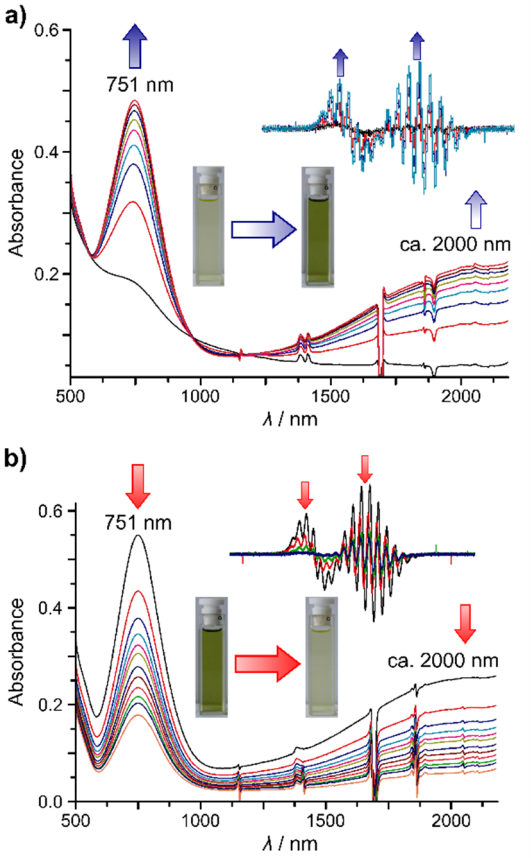

Fig. 28 UV-Vis-NIR spectroscopic changes of (a) **3** (30 μM in $CHCl_3$ at RT) with an equimolar amount of $BIQ^{2+}2PF_6^-$ titrated with increasing quantities of THACl (0–10 equiv.). Inset shows EPR spectra of **3** (0.11 mM in $CHCl_3$ at RT) with an equimolar amount of $BIQ^{2+}2PF_6^-$ titrated with increasing quantities of THACl. (b) BET upon addition of TEACl to a 1:1 mixture of **3** and $BIQ^{2+}2Cl^-$ (30 μM each in $CHCl_3$ at RT). Inset shows EPR spectra of **3** (0.11 mM in $CHCl_3$ at RT) with an equimolar amount of $BIQ^{2+}2Cl^-$ titrated with increasing quantities of TEACl (0–5 equiv.). From Ref. 68. Reprinted with permission from AAAS.

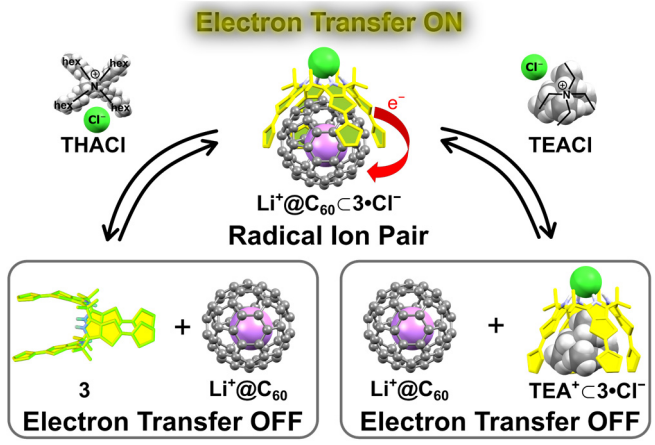

Fig. 29 Illustration of the ion-controlled ON-OFF switch of ET from **3** to $Li^+@C_{60}$. Upon addition of THACl to a mixture of **3** and $Li^+@C_{60}$ a favourable cone-conformation of Cl^-•**3** is formed allowing for the capture of $Li^+@C_{60}$ within the cavity. Addition of TEACl to this complex instigates a competition between TEA^+ and $Li^+@C_{60}$ for the cavity of Cl^-•**3** thereby turning off the ET process.

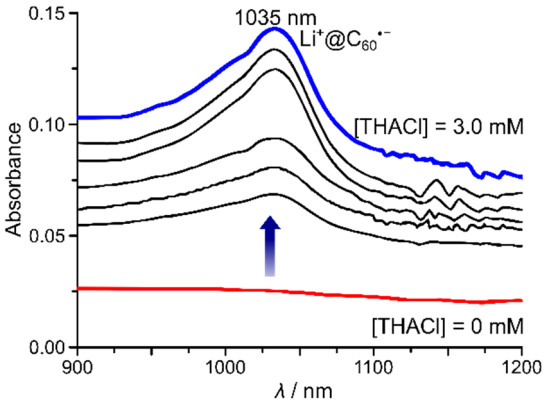

Fig. 30 NIR absorption spectroscopic changes of a solution of equimolar amounts of **3** (50 μM in PhCN at 298 K) and $[Li^+@C_{60}]PF_6$ upon addition of increasing amounts of THACl. Adapted with permission from Ref. 68. Copyright 2011 American Chemical Society.

to the cone conformation. THA^+ is large and, unlike smaller TAA^+ cations, is not bound appreciably within the bowl-like cavity produced upon conversion to the cone conformer. As a result, BIQ^{2+} is able to interact positively with **3** resulting in formation of a capsule-like self-assembled complex ($BIQ^{2+}\subset[\mathbf{3}\bullet X^-]_2$) that encloses one equiv. of BIQ^{2+}. This binding event gives rise to a colour change from pale yellow to green. The emergence of absorption bands at $\lambda = 751$ nm and $\lambda \approx 2000$ nm are seen, while the original **3** band centred at $\lambda = 329$ nm gradually disappears. These colourimetric changes are ascribed to ET from **3** to BIQ^{2+} and formation of the radical species $\mathbf{3}^{\bullet+}$ and $BIQ^{\bullet+}$. Both radical species are positively charged and diffuse away from one another leading to formation of a long-lived charge transfer state. The radical species could also be observed via EPR spectroscopy (Fig. 28); specifically, two radical signals associated with the $TTF^{\bullet+}$ radical cation (g = 2.0083) and the $BIQ^{\bullet+}$ radical cation (g = 2.0056) are easily seen. Evidence for triplet formation was also inferred from EPR spectral analyses.

Addition of smaller TAA^+ cations, such as TEA^+, to the mixture leads to a back electron transfer (BET) to produce a new neutral species $TEA^+\subset\mathbf{3}\bullet X^-$ and release of BIQ^{2+} as the result of competitive binding of the cation within the C[4]P cavity. This leads to restoration of the original pale-yellow colour. To probe the effect of cation size on the inhibition of the ET process, TEA^+, TBA^+ and THA^+ chloride salts were studied. The smaller cations had a more profound effect on the ET process with the trend for ET inhibition $TEA^+ > TBA^+ > THA^+$. A general washing with water resulted in regeneration of the original ET state. Support for the conclusions drawn on the basis of the solution phase work came from X-ray crystallographic analyses. Thus, this study served to show how substrate recognition and follow-on ET events could be modulated through the choice of small ion regulators, namely appropriately chosen anions and cations.

Elaborating on the complexation of TTF-C[4]P with fullerenes and its anion-enabled redox features, Fukuzumi *et al.*[68] demonstrated the thermal T and subsequent BET between **3** and $Li^+@C_{60}$. Again, the forward ET process was initiated via the addition of a chloride anion source (Fig. 29). This study relied on the use of $[Li^+@C_{60}]PF_6$, which is a stronger electron acceptor than pristine C_{60} as shown by CV and differential pulse voltammetry (DPV) analysis.[68] Mixing of **3** and $[Li^+@C_{60}]PF_6$ in benzonitrile (PhCN) did not result in any observed ET. Such a finding is consistent with the one-electron oxidation potential of **3** (E_{Ox} = 0.51 V vs. SCE) being higher than the one-electron reduction potential of $[Li^+@C_{60}]PF_6$ (E_{Red} = 0.14 V vs. SCE).[71]

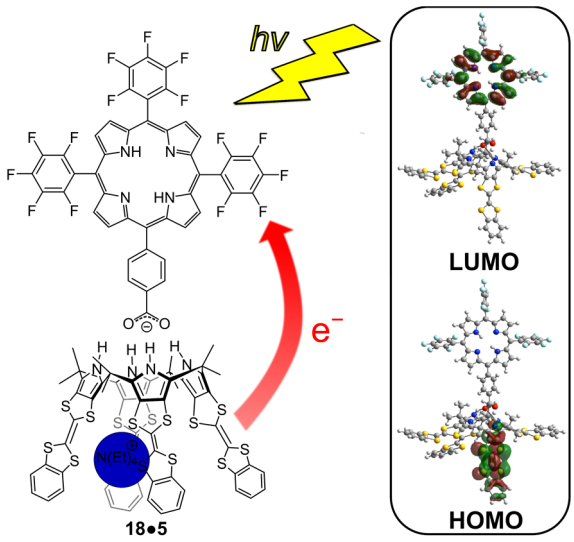

Fig. 31 Illustration of the formation of complex **18•5** as the result of hydrogen bonding between the four NH protons of **5** and the carboxylate anion. The complex is further strengthened by the complexation of TEA^+ in the cavity of **5**. Overall, this leads to favourable conditions for PET. The inset box shows the results of DFT calculations giving the frontier orbitals of the complex **18•5**. Adapted with permission from Ref. 69. Copyright 2014 American Chemical Society.

Upon the addition of THACl, ET was inferred based upon the emergence of an absorption band at λ = 1035 nm diagnostic of the $Li^+@C_{60}^{\bullet-}$ radical anion (Fig. 30). An increase in absorbance intensity was observed as more THACl was titrated into the solution, allowing an associated THACl binding constant of ~ 1.9 × 10^4 M^{-1} to be determined. A broad absorption band in the near-IR region of the spectra (diagnostic of the $[TTF\text{-}C[4]P]^{\bullet+}$ radical cation) was not observed. This led the authors to suggest that the oxidised form of **3** interacts strongly with the reduced $Li^+@C_{60}^{\bullet-}$ to form a neutral complex, instead of producing $[TTF\text{-}C[4]P]^{\bullet+}$ as a free radical cation.

EPR spectroscopic analysis of the ensemble produced from **3**, $[Li^+@C_{60}]PF_6$ and THACl revealed the presence of signals corresponding to $[\mathbf{3}]^{\bullet+}$ as would be expected following ET. Based on Density Functional Theory (DFT) calculations, this radical cation is believed to be largely localised on one TTF unit. Interestingly, no signals corresponding to $[Li^+@C_{60}]^{\bullet-}$ could be observed. This led to the conclusion that this species is characterised by a short relaxation time in solution at 298 K. Cooling the ensemble to 77 K, led to the observation of a triplet signal. Further evidence for supramolecular ensemble formation came from X-ray crystallographic analysis, which allowed the $Li^+@C_{60}\subset\mathbf{3}\bullet Cl^-$ complex to be identified.[68] As with the studies involving BIQ^{2+} detailed above, addition of TEACl to the ET ensemble resulted in a decrease of the absorption band centred at λ = 1035 nm. Again, this was interpreted in terms of cation-induced displacement of the $Li^+@C_{60}$ guest by the TEA^+ cation and BET from $[Li^+@C_{60}]^{\bullet-}$ to $[\mathbf{3}]^{\bullet+}$.

Subsequently, Sessler and co-workers explored the PET between the benzoannulated TTF-C[4]P **5** and a TEA^+ porphyrin carboxylate **18** (Fig. 31).[69] In this supramolecular system, the carboxylate moiety of **18** can interact via hydrogen bonds with TTF-C[4]P **5** in its cone conformation as previously reported.[35] The TEA^+ salt of **18** in PhCN was then titrated with **5**. An increase in absorption in the region of 400–700 nm was observed.

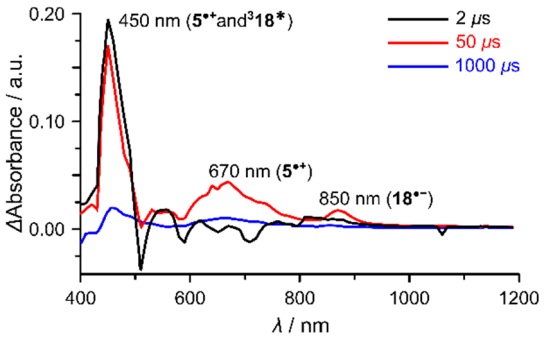

Fig. 32 Nanosecond flash photolysis absorption spectra for a mixture of **5** (0.3 mM) and **18** (0.10 mM) in PhCN at 298 K upon excitation at λ = 532 nm. Spectra recorded after 2 μs (black), 50 μs (red) and 1000 μs (blue). Adapted with permission from Ref. 69. Copyright 2014 American Chemical Society.

However, no CT band was seen at 700 nm or above, a finding interpreted in terms of a lack of appreciable electronic interaction in the ground states of **5** and **18**. ITC analysis provided support for the formation of a 1:1 complex between **5** and **18** in PhCN with an estimated binding constant of 6.3 × 10^4 M^{-1}.[69] DFT calculations of the **18•5** complex (Fig. 31) revealed that the HOMO is largely localised on the four TTF units of **5**, while the LUMO is localised on the porphyrin core of **18**. Such findings provide an electronic basis for the observed PET.

Fluorescence lifetime measurements were used to determine whether the ET occurred via a singlet or triplet excited state. Here, the lifetime of **18** was estimated to 13.4 ns. The same value was found for the **18•5** complex, indicating that the ET occurs through the triplet state.

Femtosecond transient absorption spectroscopic studies of **18•5** (50 μM each) in PhCN at 298 K were carried out with irradiation at λ = 400 nm. This revealed absorption bands at λ = 620 and 670 nm that are diagnostic of the singlet-excited state of **18**. In experiments involving the individual components and the supramolecular complex, no significant changes in decay profiles were observed. This led to the conclusion that no ET occurs to the singlet-excited state of **18**.

Under conditions of nanosecond transient absorption spectroscopy (Fig. 32), wherein a solution of **5** (0.3 mM) and **18** (0.10 mM) in PhCN was irradiated at λ = 532 nm, an increase in the absorption intensity was observed at λ = 450, 670 and 850 nm. These spectral changes correspond to formation of a joint triplet-excited state of **18** and **5**, the radical cation of **5**, and the radical anion of **18**, respectively. Analysis of the concentration-dependent behaviour revealed an intramolecular forward ET rate of 2.1 × 10^4 s^{-1}. EPR spectroscopic studies of **18•5** revealed no significant EPR signals in the absence of irradiation. On the other hand, photoirradiation with a 1000 W Hg high-pressure lamp gave rise to signals at g = 2.005 and g = 2.0067, corresponding to the radical anion of **18** (g = 2.0037) and the radical cation of **5**, respectively.[72]

Sessler and co-workers also studied the interactions between **5** and $Li^+@C_{60}$.[70] Here, they exploited the binding of fullerenes that is favoured when the counter cation is large. Thus, using another porphyrin carboxylate **19** with a THA^+ counter cation to avoid competitive binding in the cavity of the cone conformer of **5** (Fig. 33), allowed formation of a three-component supramolecular triad. Upon mixing of **5** and

$[Li^+@C_{60}]PF_6^-$ in PhCN, no changes were observed in the absorption spectrum, thus leading to the inference that no ground state ET was occurring. However, when **19** (as its THA^+ salt) was titrated into the mixture of **5** and $[Li^+@C_{60}]PF_6^-$, absorption bands appear at λ = 900 and 1035 nm indicative of the radical species $\mathbf{5}^{\bullet+}$ and $Li^+@C_{60}^{\bullet-}$, respectively. When one equiv. of **19** is titrated, the absorption bands reach a maximum value signifying complete ET between **5** and $Li^+@C_{60}$. Upon further addition of **19** a decrease in spectral intensity is seen, leading to the conclusion that the THA^+ cation starts to outcompete the binding of $Li^+@C_{60}$ within the cavity of **5**. However, under appropriately chosen conditions a supramolecular charge-separated complex consisting of $\mathbf{19}/\mathbf{5}^{\bullet+}/Li^+@C_{60}^{\bullet-}$, where the porphyrin remains in its neutral state, could be produced.

EPR spectra taken after the proposed initial ET event were characterised by signals at g = 2.0064 and g = 2.0006 corresponding to the TTF and fullerene radicals, respectively. Upon photo-irradiation, a new signal at g = 2.0028 was observed, which is attributed to the radical cation of the porphyrin carboxylate.[70] These findings support the formation of a $\mathbf{19}^{\bullet+}/\mathbf{5}/Li^+@C_{60}^{\bullet-}$ CS state.

Nanosecond laser excitation and transient absorption spectroscopy were used to obtain further insights into the underlying events. Excitation at λ = 532 nm led to the production of transient absorption bands at λ = 440 and 790 nm with bleaching occurring at λ = 650 and 720 nm. The band at λ = 440 nm is attributed to the triplet excited state of the porphyrin $^3\mathbf{19}^*$. This feature decayed as the band at λ = 790 nm ($\mathbf{19}^{\bullet+}$) increased while the bleaching bands recovered.[70] These findings were taken as an indication that under these conditions ET from the porphyrin **19** to the TTF-C[4]P **5** occurs. No changes in the absorbance attributed to $Li^+@C_{60}^{\bullet-}$ (λ = 1035 nm) were seen, leading the authors to conclude that that $Li^+@C_{60}^{\bullet-}$ remains unchanged with and without photoexcitation. The decay of the absorption bands attributed to $\mathbf{5}^{\bullet+}$ support the formation of a higher energy CS state where the charges are localised on **19** and $Li^+@C_{60}$ within $\mathbf{19}^{\bullet+}/\mathbf{5}/Li^+@C_{60}^{\bullet-}$. This study thus demonstrates another way in which the recognition events associated with TTF-C[4]Ps may be used to control ET processes.

The introduction of specific anions and cations to modulate the redox features of TTF-C[4]Ps was used by Sessler, Park and collaborators to control two disparate downstream chemical reactions.[71] In this recent study, a strong electron acceptor, namely TCNQ, was used in conjunction with TTF-C[4]P **5**. Solid state analyses revealed that **5** and TCNQ form a 1:2 host guest complex in the solid state (Fig. 34). In solution, these latter interactions are manifested in terms of a change in colour from yellow (**5**) to dark brown (**5** + TCNQ) and the appearance of a broad absorption feature centred at ca. 1400 nm. A controlled change in the complex behaviour could be effected by choosing specific ionic salts. For instance, adding TEACl to the solution containing the complex produced a dramatic change in the spectral features. As recognised from prior work[67,68] described earlier in this review, the complexation of TTF-C[4]P with TEACl results in a formation of a relatively strong complex $TEA^+\subset$TTF-C[4]P$\bullet Cl^-$ where the TEA^+ is situated inside the cavity of the C[4]P receptor in its cone conformation. The competition between TCNQ and TEACl favours TEACl. TCNQ is thus released from the complex returning the colour of the mixture to its original yellow (Fig. 35). Changing the TEA^+ cation to a bulkier THA^+ precludes formation of a cation-bound complex. However, the anion remains bound. This gives complex $\mathbf{5}\bullet Cl^-$ with the THA^+ cation situated outside the cavity of the TTF-C[4]P receptor, which remains in its cone conformation. Coupled with the chloride-induced anodic shift of **5** (ΔE_1 = 60 mV) this permits ET between **5** and TCNQ and formation of two radical species, namely $[\mathbf{5}]^{\bullet+}\bullet Cl^-$ and $[TCNQ]^{\bullet-}$. This conversion leads to a green colour and produces absorption bands centered at λ = 650 nm, 750 nm, and λ = 850 nm in the UV-Vis-NIR absorption spectrum that are attributed to formation of $[TCNQ]^{\bullet-}$.[72] This controlled

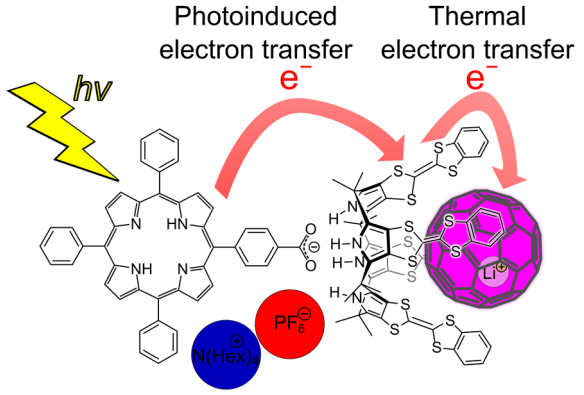

Fig. 33 Complex $Li^+@C_{60}\subset\mathbf{5}\bullet\mathbf{19}$ formed when the counter cation (in blue) is THA^+. In this ensemble permits both thermal ET between **5** and $Li^+@C_{60}$ and PET from the porphyrin (**19**) to the TTF-C[4]P.

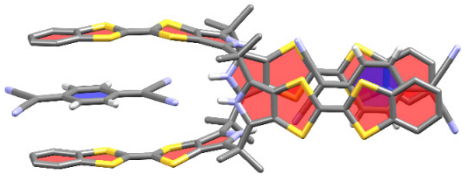

Fig. 34 Single-crystal X-ray structure of the complex $TCNQ_2\subset\mathbf{5}$ obtained by slow evaporation of a 1:2 CH_3Cl solution of **5** and TCNQ, respectively. CH_3Cl and CH hydrogens on **5** have been removed for clarity.[71]

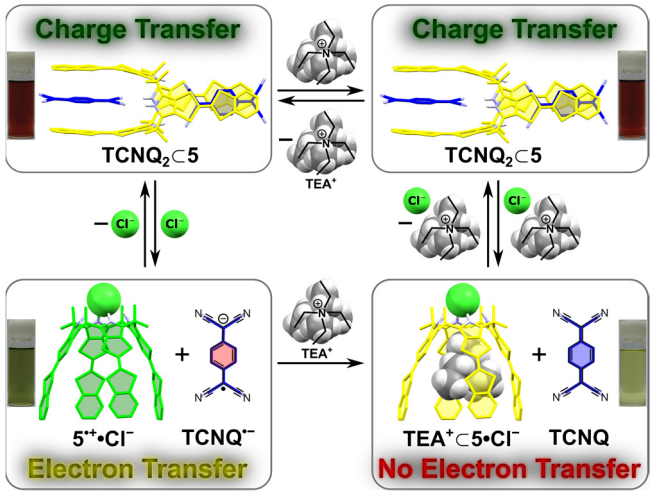

Fig. 35 Illustration of the ionically controlled supramolecular tristate switching operation by selective addition of cation (TEA^+) and anion (Cl^-) pairs to stabilise three limiting states, involving charge transfer ("Hi-Z" state), ET ("1" state) or no ET ("0" state). Adapted with permission from Ref. 71. Copyright 2018 American Chemical Society.

switching can be regarded as a tristate buffer that permits access to three different states, referred to as the "0"(No ET), "1" (ET) and "Hi-Z" (CT) states in loose analogy to the terms used in microelectronics. Control experiments using $TEABF_4$ did not result in a change from the "Hi-Z" or charge transfer state due to the non-coordinating nature of the BF_4^- anion, thereby underscoring the need to have both ionic inputs present to achieve full ET.

The ability to access three distinct states by carefully choosing the appropriate cation and anion led the authors to suggest that the system could be used to control different downstream cascade-type reactions.[71] As a first test of this suggestion, the system consisting of (**5** + TCNQ) was explored as a radical initiator for the polymerisation of styrene to polystyrene. Specifically, mixtures of **5** and TCNQ in styrene were monitored by absorption and ^{1}H NMR spectroscopy under conditions expected to favour formation of the three output states. Only the "1" ET state results in radical-based polymerisation, as inferred from ^{1}H NMR spectral analyses. No polystyrene was observed under any other conditions tested. This conclusion was supported by UV-Vis-NIR spectroscopic studies. Spectra recorded immediately after mixing **5** + TCNQ and styrene revealed absorption bands (λ = 855 nm) corresponding to the radical "1" state only when THACl was also present, but not in the case of any of the other inputs.

Having shown the control of a radical reaction by addition of two upstream ionic stimuli that do not affect it directly, the authors further demonstrated a second example of "chemical communication". In this system, advantage was taken of the chemical reactivity of TCNQ by adding 4-ethynyl-*N*,*N*-dimethylaniline to the system. This latter alkyne is known to undergo a cycloaddition and subsequent retroelectrocyclisation reaction in the presence of TNCQ. Under conditions favouring the "0" (No ET) state, formation of product is observed, as inferred from absorption and ^{1}H NMR spectroscopic analyses. Neither the "1" nor "Hi-Z" states produced any observable product. Taken in conjunction with the styrene polymerisation study, this finding was taken as support for the notion that this tristate buffer system could be used to control the release of "chemical messengers" that could be used to modulate downstream reactions.

Given the progress made to date, we believe that chemical control over conformation, cavity shape, and the first oxidation potential of TTF-C[4]P allows for the creation of complex, multicomponent supramolecular systems can be used to modify the electronic structure of the system and promote reactions that exploit differences in CT, ET, and BET effects. This can allow for creation of rationally designed chemical communication cascades.

Conclusions

To date, the diverse interactions of TTF-C[4]Ps with a range of substrates have led to the construction of a number of intricate systems comprising stimuli-controlled complexation of electron-deficient guests, as well as stimuli-controlled electron-transfer events. The dynamic nature of this set of receptors parallels some of the features of natural receptors, in particular the cooperative binding of both homologous and heterologous guests. These features have recently been exploited in ensembles for chemical communication wherein binding events are used to control downstream chemical reactions.

TTF-C[4]Ps and related systems have also been exploited for the colorimetric detection of nitroaromatic explosives, substrates for which the formation of complexes with 1:2 host guest stoichiometry are often observed. Binding-induced modulation of the electronic features of the receptor system, including in particular that of the TTF moieties, allows the complexation strength to be modulated as a consequence of tuning the electron donating properties and adjusting the steric hindrance associated with substrate recognition.

Overall, TTF-C[4]Ps have been shown to be unique binding motifs wherein changes in the number of TTF units and in the macrocycle can lead to dramatic changes in the complexation features. We thus believe that TTF-C[n]Ps hold considerable promise as components in sensing devices and as building blocks for functional ensembles. Work is ongoing in our laboratories in an effort to realise this promise.

Acknowledgements

SB acknowledges the Danish Council for Independent Research, Technology and Production Sciences (FTP, 5054-00052). The work in Austin was supported by the National Science Foundation (CHE-1807152 to JLS) and the Robert A. Welch Foundation (F-0018 to JLS). JOJ thanks the Villum Foundation and the Danish Natural Science Research Council (FNU, Project 11-106744) for financial support.

Notes and references

§ The *n* of the Hill coefficient is not to be confused with the n used to designate the number of pyrrolic substituents in calix[n]pyrroles.

1 J. O. Jeppesen, K. Takimiya, F. Jensen and J. Becher, *Org. Lett.*, 1999, **1**, 1291–1294.
2 J. O. Jeppesen, K. Takimiya, F. Jensen, T. Brimert, K. Nielsen, N. Thorup and J. Becher, *J. Org. Chem.*, 2000, **65**, 5794–5805.
3 A. Baeyer, *Ber. Dtsch. Chem. Ges.*, 1886, **19**, 2184–2185.
4 P. A. Gale, J. L. Sessler, V. Král and V. Lynch, *J. Am. Chem. Soc.*, 1996, **118**, 5140-5141.
5 S. K. Kim and J. L. Sessler, *Acc. Chem. Res.*, 2014, **47**, 2525–2536.
6 I. Saha, J. T. Lee and C.-H. Lee, *Eur. J. Org. Chem.*, 2015, **2015**, 3859–3885.
7 Q. He, M. Kelliher, S. Bähring, V. L. Lynch and J. L. Sessler, *J. Am. Chem. Soc.*, 2017, **139**, 7140–7143.
8 P. Anzenbacher, A. C. Try, H. Miyaji, K. Jursíková, V. M. Lynch, M. Marquez and J. L. Sessler, *J. Am. Chem. Soc.*, 2000, **122**, 10268–10272.
9 S. K. Kim, D. E. Gross, D.-G. Cho, V. M. Lynch and J. L. Sessler, *J. Org. Chem.*, 2011, **76**, 1005–1012.
10 I. Saha, K. H. Park, M. Han, S. K. Kim, V. M. Lynch, J. L. Sessler and C.-H. Lee, *Org. Lett.*, 2014, **16**, 5414–5417.
11 W. R. H. Hurtley and S. Smiles, *J. Chem. Soc.*, 1926, **129**, 2263–2270.

12 F. Wudl, G. M. Smith and E. J. Hufnagel, *J. Chem. Soc. D.*, 1970, 1453–1454.
13 A. Andrieux, C. Duroure, D. Jérome and K. Bechgaard, *J. Phys. Lett.*, 1979, **40**, 381–383.
14 D. Jérome, A. Mazaud, M. Ribault and K. Bechgaard, *J. Phys. Lett.*, 1980, **41**, 95–98.
15 S. S. P. Parkin, E. M. Engler, R. R. Schumaker, R. Lagier, V. Y. Lee, J. C. Scott and R. L. Greene, *Phys. Rev. Lett.*, 1983, **50**, 270–273.
16 J. Becher, Z. T. Li, P. Blanchard, N. Svenstrup, J. Lau, M. B. Nielsen and P. Leriche, *Pure Appl. Chem.*, 1997, **69**, 465–470.
17 T. Jørgensen, T. K. Hansen and J. Becher, *Chem. Soc. Rev.*, 1994, **23**, 41–51.
18 M. R. Bryce, *J. Mater. Chem.*, 1995, **5**, 1481–1496.
19 M. R. Bryce, *J. Mater. Chem.*, 2000, **10**, 589–598.
20 M. B. Nielsen, C. Lomholt and J. Becher, *Chem. Soc. Rev.*, 2000, **29**, 153–164.
21 J. L. Segura and N. Martin, *Angew. Chem., Int. Ed.*, 2001, **40**, 1372–1409.
22 D. Canevet, M. Sallé, G. Zhang, D. Zhang and D. Zhu, *Chem. Commun.*, 2009, **0**, 2245–2269.
23 J. S. Park, K. Y. Yoon, D. S. Kim, V. M. Lynch, C. W. Bielawski, K. P. Johnston and J. L. Sessler, *Proc. Natl. Acad. Sci. U. S. A.*, 2011, **108**, 20913–20917.
24 D. S. Kim, V. M. Lynch, J. S. Park and J. L. Sessler, *J. Am. Chem. Soc.*, 2013, **135**, 14889–14894.
25 S. Bähring, D. S. Kim, T. Duedal, V. M. Lynch, K. A. Nielsen, J. O. Jeppesen and J. L. Sessler, *Chem. Commun.*, 2014, **50**, 5497-5499.
26 D. S. Kim, J. Chang, S. Leem, J. S. Park, P. Thordarson and J. L. Sessler, *J. Am. Chem. Soc.*, 2015, **137**, 16038–16042.
27 S. Bähring, L. Martin-Gomis, G. Olsen, K. A. Nielsen, D. S. Kim, T. Duedal, A. Sastre-Santos, J. O. Jeppesen and J. L. Sessler, *Chem. - Eur. J.*, 2016, **22**, 1958–1967.
28 Y. Liu, A. H. Flood, P. A. Bonvallett, S. A. Vignon, B. H. Northrop, H. R. Tseng, J. O. Jeppesen, T. J. Huang, B. Brough, M. Baller, S. Magonov, S. D. Solares, W. A. Goddard, C. M. Ho and J. F. Stoddart, *J. Am. Chem. Soc.*, 2005, **127**, 9745–9759.
29 B. K. Juluri, A. S. Kumar, Y. Liu, T. Ye, Y.-W. Yang, A. H. Flood, L. Fang, J. F. Stoddart, P. S. Weiss and T. J. Huang, *ACS Nano*, 2009, **3**, 291–300.
30 A. Coskun, M. Banaszak, R. D. Astumian, J. F. Stoddart and B. A. Grzybowski, *Chem. Soc. Rev.*, 2012, **41**, 19–30.
31 C. J. Bruns and J. F. Stoddart, *Acc. Chem. Res.*, 2014, **47**, 2186–2199.
32 A. Jana, M. Ishida, J. S. Park, S. Bähring, J. O. Jeppesen and J. L. Sessler, *Chem. Rev.*, 2017, **117**, 2641–2710.
33 A. Jana, S. Bähring, M. Ishida, S. Goeb, D. Canevet, M. Sallé, J. O. Jeppesen and J. L. Sessler, *Chem. Soc. Rev.*, 2018, **47**, 5614–5645.
34 K. A. Nielsen, J. O. Jeppesen, E. Levillain and J. Becher, *Angew. Chem., Int. Ed.*, 2003, **42**, 187–191.
35 K. A. Nielsen, W.-S. Cho, J. Lyskawa, E. Levillain, V. M. Lynch, J. L. Sessler and J. O. Jeppesen, *J. Am. Chem. Soc.*, 2006, **128**, 2444–2451.
36 L. G. Jensen, K. A. Nielsen, T. Breton, J. L. Sessler, J. O. Jeppesen, E. Levillain and L. Sanguinet, *Chem. Eur. J.*, 2009, **15**, 8128–8133.
37 W. E. Allen, P. A. Gale, C. T. Brown, V. M. Lynch and J. L. Sessler, *J. Am. Chem. Soc.*, 1996, **118**, 12471–12472.
38 J. R. Blas, J. M. López-Bes, M. Márquez, J. L. Sessler, F. J. Luque and M. Orozco, *Chem. Eur. J.*, 2007, **13**, 1108–1116.
39 K. A. Nielsen, W.-S. Cho, J. O. Jeppesen, V. M. Lynch, J. Becher and J. L. Sessler, *J. Am. Chem. Soc.*, 2004, **126**, 16296–16297.
40 C. A. Hunter and J. K. M. Sanders, *J. Am. Chem. Soc.*, 1990, **112**, 5525–5534.
41 T. Duedal, K. A. Nielsen, G. Olsen, C. B. G. Rasmussen, J. Kongsted, E. Levillain, T. Breton, E. Miyazaki, K. Takimiya, S. Bähring and J. O. Jeppesen, *J. Org. Chem.*, 2017, **82**, 2123–2128.
42 K. A. Nielsen, W.-S. Cho, G. H. Sarova, B. M. Petersen, A. D. Bond, J. Becher, F. Jensen, D. M. Guldi, J. L. Sessler and J. O. Jeppesen, *Angew. Chem. Int. Ed.*, 2006, **45**, 6848–6853.
43 P. Job, *Annales De Chimie France*, 1928, **9**, 113–203.
44 C. M. Davis, J. M. Lim, K. R. Larsen, D. S. Kim, Y. M. Sung, D. M. Lyons, V. M. Lynch, K. A. Nielsen, J. O. Jeppesen, D. Kim, J. S. Park and J. L. Sessler, *J. Am. Chem. Soc.*, 2014, **136**, 10410–10417.
45 D. M. Guldi and M. Prato, *Acc. Chem. Res.*, 2000, **33**, 695–703.
46 M. h. Chahma, X. Wang, A. van der Est and M. Pilkington, *J. Org. Chem.*, 2006, **71**, 2750–2755.
47 K. A. Nielsen, L. Martín-Gomis, G. H. Sarova, L. Sanguinet, D. E. Gross, F. Fernández-Lázaro, P. C. Stein, E. Levillain, J. L. Sessler, D. M. Guldi, Á. Sastre-Santos and J. O. Jeppesen, *Tetrahedron*, 2008, **64**, 8449–8463.
48 J. S. Park, C. Bejger, K. R. Larsen, K. A. Nielsen, A. Jana, V. M. Lynch, J. O. Jeppesen, D. Kim and J. L. Sessler, *Chem. Sci.*, 2012, **3**, 2685–2689.
49 G. Cafeo, F. H. Kohnke, G. L. L. Torre, A. J. P. White and D. J. Williams, *Angew. Chem. Int. Ed.*, 2000, **39**, 1496–1498.
50 J. S. Park, F. Le Derf, C. M. Bejger, V. M. Lynch, J. L. Sessler, K. A. Nielsen, C. Johnsen and J. O. Jeppesen, *Chem. Eur. J.*, 2010, **16**, 848–854.
51 J. Monod, J.-P. Changeux and F. Jacob, *J. Mol. Biol.*, 1963, **6**, 306–329.
52 M. F. Perutz, G. Fermi, B. Luisi, B. Shaanan and R. C. Liddington, *Acc. Chem. Res.*, 1987, **20**, 309–321.
53 G. S. Adair, W. t. c. o. A. V. Bock and J. H. Field, *J. Biol. Chem.*, 1925, **63**, 529–545.
54 T. L. Hill, *Cooperativity Theory in Biochemistry. Steady-State and Equilibrium Systems*, Springer, New York, 1985.
55 W. B. Zhu, J. S. Park, J. L. Sessler and A. Gaitas, *Appl. Phys. Lett.*, 2011, **98**.
56 F. G. Bosco, M. Bache, E. T. Hwu, C. H. Chen, S. S. Andersen, K. A. Nielsen, S. S. Keller, J. O. Jeppesen, I. S. Hwang and A. Boisen, *Sens. Actuators, B*, 2012, **171–172**, 1054–1059.
57 E. H. Witlicki, S. Bähring, C. Johnsen, M. V. Solano, K. A. Nielsen, D. W. Silverstein, C. W. Marlatt, L. Jensen, J. O. Jeppesen and A. H. Flood, *Chem. Commun.*, 2017, **53**, 10918–10921.
58 T. Poulsen, K. A. Nielsen, A. D. Bond and J. O. Jeppesen, *Org. Lett.*, 2007, **9**, 5485–5488.
59 D.-S. Kim, V. M. Lynch, K. A. Nielsen, C. Johnsen, J. O. Jeppesen and J. L. Sessler, *Anal. Bioanal. Chem.*, 2009, **395**, 393–400.
60 K. A. Nielsen, S. Bähring and J. O. Jeppesen, *Chem. Eur. J.*, 2011, **17**, 11001–11007.
61 T. Fehrentz, M. Schönberger and D. Trauner, *Angew. Chem. Int. Ed.*, 2011, **50**, 12156–12182.
62 S. Liu, C. Ruspic, P. Mukhopadhyay, S. Chakrabarti, P. Y. Zavalij and L. Isaacs, *J. Am. Chem. Soc.*, 2005, **127**, 15959–15967.
63 K. A. Nielsen and P. C. Stein, *Org. Lett.*, 2011, **13**, 6176–6179.
64 K. A. Nielsen, *Tetrahedron Lett.*, 2012, **53**, 5616–5618.
65 S. Bähring, G. Olsen, P. C. Stein, J. Kongsted and K. A. Nielsen, *Chem. Eur. J.*, 2013, **19**, 2768–2775.
66 L. Fielding, *Tetrahedron*, 2000, **56**, 6151–6170.
67 J. S. Park, E. Karnas, K. Ohkubo, P. Chen, K. M. Kadish, S. Fukuzumi, C. W. Bielawski, T. W. Hudnall, V. M. Lynch and J. L. Sessler, *Science*, 2010, **329**, 1324–1327.
68 S. Fukuzumi, K. Ohkubo, Y. Kawashima, D. S. Kim, J. S. Park, A. Jana, V. M. Lynch, D. Kim and J. L. Sessler, *J. Am. Chem. Soc.*, 2011, **133**, 15938–15941.

69 C. M. Davis, Y. Kawashima, K. Ohkubo, J. M. Lim, D. Kim, S. Fukuzumi and J. L. Sessler, *J. Phys. Chem. C*, 2014, **118**, 13503–13513.
70 C. M. Davis, K. Ohkubo, A. D. Lammer, D. S. Kim, Y. Kawashima, J. L. Sessler and S. Fukuzumi, *Chem. Commun.*, 2015, **51**, 9789–9792.
71 J. S. Park, J. Park, Y. J. Yang, T. T. Tran, I. S. Kim and J. L. Sessler, *J. Am. Chem. Soc.*, 2018, **140**, 7598–7604.
72 G. Wang, X. Fu, J. Deng, X. Huang and Q. Miao, *Chem. Phys. Lett.*, 2013, **579**, 105–110.

Author Biography

Steffen Bähring received his Ph.D. in Supramolecular Chemistry from the University of Southern Denmark in 2013 under the guidance of Professors Kent A. Nielsen and Jan O. Jeppesen. During this time, he visited the Sessler lab (2011–2012). After his Ph.D., he worked at the Danish Technological Institute as an R&D consultant for the Oil & Gas industry. Dr. Bähring was awarded a Danish Independent Postdoctoral Scholarship to work on tetrathiafulvalene-based organic photovoltaics. In 2018, he became an Assistant Professor at the University of Southern Denmark.

Harrison D. Root graduated Cum Laude with a B.S. in professional chemistry with a minor in mathematics from the University of Nevada, Reno before beginning his Ph.D. studies in supramolecular chemistry under the tutelage of Professor Jonathan L. Sessler at the University of Texas at Austin. His studies at University of Texas at Austin center around tetrathiafulvalene-containing macrocycles.

Jonathan L. Sessler received a B.Sc. degree in Chemistry in 1977 from the University of California, Berkeley. He obtained his Ph.D. from Stanford University in 1982. He was an NSF-NATO and NSF-CNRS Postdoctoral Fellow at Université Louis Pasteur de Strasbourg (1982–1983). In 1984 he accepted a position as an Assistant Professor of Chemistry at the University of Texas at Austin, where he is currently the Doherty-Welch Chair. Professor Sessler is currently the Director of the Center for Supramolecular Chemistry and Catalysis at Shanghai University.
http://sessler.cm.utexas.edu/Sessler_Group_Website/Home.html

Jan O. Jeppesen received his B.Sc., M.Sc., and Ph.D. degrees in 1996, 1999, and 2001, respectively, from the University of Southern Denmark for work in supramolecular tetrathiafulvalene chemistry. In the first part of his Ph.D. studies, he developed a synthetic route to pyrrolo-tetrathiafulvalenes and in 2000-2001, he joined the group of Professor Sir Fraser Stoddart at the University of California, Los Angeles (UCLA) working on the design and synthesis of amphiphilic bistable [2]rotaxanes. Since 2008, he has been a Full Professor at the University of Southern Denmark, and in 2018 he was knighted by the Majesty Queen Margrethe II of Denmark.
http://www.jojgroup.sdu.dk

Table of Contents

Tetrakis-tetrathiafulvalene-calix[4]pyrrole: A versatile synthetic receptor for electron-deficient planar and spherical guests Steffen Bähring,[a]* Harrison D. Root,[b] Jonathan L. Sessler[b]* and Jan O. Jeppesen[a]*

[a] Department of Physics, Chemistry and Pharmacy, University of Southern Denmark, Campusvej 55, 5230, Odense M, Denmark. E-mail: sbahring@sdu.dk; joj@sdu.dk

[b] Department of Chemistry, The University of Texas at Austin, Austin, Texas 78712-1224, USA. E-mail: Sessler@cm.utexas.edu